MARTIN MARIETTA ENERGY SYSTEMS LIBRARIES
3 4456 0365942 2

ORNL-3468
UC-34 – Physics
TID-4500 (21st ed.)

# OPTICAL EMISSION FROM ELECTRON IRRADIATED THIN GOLD FOILS

(Thesis)

D. C. Hammer
E. T. Arakawa
L. C. Emerson
R. D. Birkhoff

**OAK RIDGE NATIONAL LABORATORY**
operated by
UNION CARBIDE CORPORATION
for the
U.S. ATOMIC ENERGY COMMISSION

CENTRAL RESEARCH LIBRARY
DOCUMENT COLLECTION
**LIBRARY LOAN COPY**
DO NOT TRANSFER TO ANOTHER PERSON
If you wish someone else to see this document, send in name with document and the library will arrange a loan.

LEGAL NOTICE

This report was prepared as an account of Government sponsored work. Neither the United States, nor the Commission, nor any person acting on behalf of the Commission:

A. Makes any warranty or representation, expressed or implied, with respect to the accuracy, completeness, or usefulness of the information contained in this report, or that the use of any information, apparatus, method, or process disclosed in this report may not infringe privately owned rights; or

B. Assumes any liabilities with respect to the use of, or for damages resulting from the use of any information, apparatus, method, or process disclosed in this report.

As used in the above, "person acting on behalf of the Commission" includes any employee or contractor of the Commission, or employee of such contractor, to the extent that such employee or contractor of the Commission, or employee of such contractor prepares, disseminates, or provides access to, any information pursuant to his employment or contract with the Commission, or his employment with such contractor.

ORNL-3468

Contract No. W-7405-eng-26

HEALTH PHYSICS DIVISION

# OPTICAL EMISSION FROM ELECTRON IRRADIATED THIN GOLD FOILS

D. C. Hammer, E. T. Arakawa, L. C. Emerson,
and R. D. Birkhoff

(Submitted by D.C.H. as a thesis to the Faculty of the Graduate School of Vanderbilt University in partial fulfillment of the requirements for the degree of Master of Science in Physics)

Date Issued

AUG 26 1963

OAK RIDGE NATIONAL LABORATORY
Oak Ridge, Tennessee
operated by
UNION CARBIDE CORPORATION
for the
U. S. ATOMIC ENERGY COMMISSION

MARTIN MARIETTA ENERGY SYSTEMS LIBRARIES

3 4456 0365942 2

## ACKNOWLEDGMENTS

The authors wish to express their appreciation to J. L. Feuerbacher for his help in evaluating the Ritchie-Eldridge theory on the digital computer and to J. A. Harter and D. C. Pittman for their help on electronic problems which arose during this work.

# TABLE OF CONTENTS


| | Page |
|---|---|
| ACKNOWLEDGMENTS | ii |
| LIST OF TABLES | iv |
| LIST OF FIGURES | v |
| ABSTRACT | vi |
| I. INTRODUCTION | 1 |
| II. THEORY | 4 |
| A. Plasma Radiation | |
| B. Transition Radiation | |
| C. Bremsstrahlung | |
| III. APPARATUS | 9 |
| A. Introduction and General Description | |
| B. Accelerator | |
| C. Electron Gun | |
| D. Irradiation Chamber | |
| E. Spectrometer | |
| F. Polarizer | |
| G. Current Measuring Instruments | |
| H. Vacuum System | |
| IV. THIN FOIL PREPARATION AND THICKNESS DETERMINATION | 16 |
| A. Foil Preparation | |
| B. Determination of Foil Thickness | |
| V. CALIBRATION OF APPARATUS | 27 |
| A. Calibration with a Standard Light Source | |
| B. Calibration in the Far Ultraviolet | |
| VI. RESULTS | 44 |
| VII. REVIEW AND CONCLUSIONS | 57 |
| BIBLIOGRAPHY | 59 |

# LIST OF TABLES

Table Page

1. Variation of Foil Thickness as a Function of Position on Glass Slide . . . . . 21

# LIST OF FIGURES


| Figure | | Page |
|---|---|---|
| 1. | Schematic Diagram of Accelerator, Irradiation Chamber, and Spectrometer | 10 |
| 2. | Schematic Diagram of Samples Used to Check Variation in Foil Thickness | 20 |
| 3. | Schematic Diagram of Optical Interferometer | 23 |
| 4. | Photograph of Fringe Shift for a 425-Å Thick Foil | 25 |
| 5. | Correction Factor for Spectral Response of Spectrometer | 29 |
| 6. | Photograph of Ultraviolet Spectrometer and Grating Calibrator | 35 |
| 7. | Schematic Diagram of Ultraviolet Spectrometer and Grating Calibrator | 36 |
| 8. | Absolute Efficiency of 3500-Å Blaze Grating as a Function of Wavelength | 40 |
| 9. | Absolute Efficiency of 6000-Å Blaze Grating as a Function of Wavelength | 42 |
| 10. | Absolute Efficiency of 1100-Å Blaze Grating as a Function of Wavelength | 43 |
| 11. | Spectral Distributions for 340-Å Au Foil (E = 40 keV) | 45 |
| 12. | Spectral Distributions for 340-Å Au Foil (E = 60 keV) | 46 |
| 13. | Spectral Distributions for 340-Å Au Foil (E = 80 keV) | 47 |
| 14. | Spectral Distributions for 340-Å Au Foil (E = 100 keV) | 48 |
| 15. | Spectral Distributions for 530-Å Au Foil (E = 25 keV) | 49 |
| 16. | Spectral Distributions for 530-Å Au Foil (E = 40 keV) | 50 |
| 17. | Spectral Distributions for 530-Å Au Foil (E = 60 keV) | 51 |
| 18. | Spectral Distributions for 530-Å Au Foil (E = 80 keV) | 52 |
| 19. | Spectral Distributions for 530-Å Au Foil (E = 100 keV) | 53 |
| 20. | Bremsstrahlung Yield for Gold as a Function of Beam Energy (t = 500 Å, $\lambda$ = 3500 Å) | 54 |

# ABSTRACT

The light produced in thin gold foils, 340 Å and 530 Å thick, by high energy electron bombardment has been investigated in the wavelength region between 2500 Å and 5500 Å. Monochromatic electron beams of 1.5 μa with energies between 25 and 100 keV were used in the study. The spectral distribution and the polarization characteristics of the light were determined with a Seya-Namioka vacuum ultraviolet spectrometer, Glan prism analyzer, and a 13-stage quartz window photomultiplier. The optical system was calibrated by use of a standard lamp obtained from the National Bureau of Standards.

The experimental results show that gold emits a continuous distribution of photons polarized parallel to the plane of incidence over the spectral region investigated. The spectrum is characterized by a fairly rapid decrease in photon intensity at the shorter wavelengths to a minimum at 4500 to 5000 Å followed by a gradual rise to 5500 Å. In general, the measured intensities fall in the range from 1 to 10 eV per incident electron per unit solid angle per centimeter of wavelength. The spectral distribution of photons polarized perpendicular to the plane of incidence was found to be fairly flat with intensities ranging from 10% to 20% of those of the parallel component.

The experimental results were compared with the generalized theory of transition radiation as formulated by Ritchie and Eldridge and with the low energy bremsstrahlung theory of Gluckstern, Hull, and Breit. The agreement between the measured intensities of the parallel polarized components and the calculated intensities of transition

radiation was found to be good, especially at the higher energies. The experimentally measured perpendicular components were compared with the calculated perpendicular components of optical bremsstrahlung. Although the absolute agreement was not as good as in the case of transition radiation, the inverse energy dependence predicted by the Gluckstern-Hull-Breit theory was observed. Reasons for the observed discrepancies are presented.

In the course of the experimental investigation, a calibration device was constructed with which a determination was made of the absolute efficiency of the concave diffraction gratings used in the Seya-Namioka geometry. The results of efficiency studies of several typical gratings are presented over a wide range of wavelengths.

# I. INTRODUCTION

At least three more or less distinct sources of light may contribute to the total spectral emission from thin metallic films bombarded by electrons. These are plasma radiation, transition radiation, and bremsstrahlung. Plasma radiation[1] results from the decay by photon emission of the conduction electron plasma which has been excited by fast electrons. The study of plasma effects in solids by optical methods was first proposed by Ferrell[2] in 1958 in a paper in which he calculated the expected photon yield. Transition radiation, hypothesized and treated by Frank and Ginzburg[3] in 1945, arises when an energetic electron "transits" from one medium into another. A more comprehensive theory including the effects of both plasma and transition radiation was proposed by Ritchie[4] in 1961. The theory of Ritchie and the bremsstrahlung theory of Gluckstern, Hull, and Breit[5] were used to interpret the experimental results obtained in this study.

Ferrell[6] predicted that the variation in light intensity should

---

[1] R. A. Ferrell, Phys. Rev. 111, 1214 (1958).

[2] Ibid.

[3] I. Frank and V. Ginzburg, J. Phys. (U.S.S.R.) 9, 353 (1945).

[4] R. H. Ritchie and H. B. Eldridge, Phys. Rev. 126, 1935 (1962); See also E. T. Arakawa, A. L. Frank, R. D. Birkhoff, and R. H. Ritchie, Bull. Am. Phys. Soc. 6, 266 (1961).

[5] R. L. Gluckstern, M. H. Hull, Jr., and G. Breit, Phys. Rev. 90, 1026 (1953).

[6] Ferrell, loc. cit.

depend on foil thickness, electron beam energy, and the angle of photon emission. Furthermore, the radiation should have a narrow spectral distribution at the plasma frequency, and the intensity of the radiation as a function of angle should obey a modified cos $\theta$ relation, where $\theta$ is the angle between the foil normal and the direction of emission of the photon. Ferrell stated that only for electron oscillations in the normal direction would the probability be large for radiation and further stated that no radiation would be emitted normal to the irradiated surface.

The transition radiation of Frank and Ginzburg[7] arises when an electron crosses a plane boundary between two media, usually considered to be a vacuum and a metal. Thus, when an electron enters a metal the electron and its image charge annihilate with accompanying photon emission. Frank and Ginzburg predicted that in all cases transition radiation would be completely polarized with the E vector in the plane defined by the electron beam and the direction of the radiated photon. This prediction indicated that transition radiation could be separated experimentally from bremsstrahlung (which is only slightly polarized) by use of a polarizer. In a recent paper Frank[8] stated that the intensity of transition radiation should be proportional to the particle energy and inversely proportional to the particle mass. Furthermore, the conditions for observation of transition radiation become more favorable

---

[7] Frank and Ginzburg, loc. cit.

[8] I. M. Frank, Uspekhi Fiz. Nauk. 75, 231 (1961).

as the particle energy increases for two reasons: first, the intensity increases, and second, background radiations are usually reduced. His statement that transition radiation is completely polarized in the plane of incidence involves the assumptions that scattering of the electron in the metal and any depolarization of the light due to the irregularities of the target surface can be neglected, neither of which is always valid. Frank also pointed out that the properties of transition radiation are determined by the optical constants of the target and suggested that a study of transition radiation may be very useful for determining the optical properties of various materials, particularly of metals.

## II. THEORY

### A. Plasma Radiation

The equations derived by Ferrell[9] can be combined into a single equation appropriate to the experimental situation encountered. The photon intensity $E(\theta,t,\lambda,v)$ emitted per incident electron at angle $\theta$ per unit solid angle in the wavelength interval $\lambda$ to $\lambda + d\lambda$ is given by

$$E(\theta,t,\lambda,v) = \frac{e^2\beta^2 \lambda_p \sin^2\theta \cos\theta \sin^2\left(\frac{\pi t}{\lambda_{ex}}\right)}{2\pi\left[\left(1 - \frac{\lambda_p}{\lambda}\right)^2 + \frac{1}{4}\left(2nk + \frac{\pi t \sin^2\theta}{\lambda_{ex}\cos\theta}\right)^2\right]} \qquad (1)$$

where t is the foil thickness, $\lambda_{ex} = \frac{v}{c}\lambda_p$, where $\lambda_p$ is the plasma wavelength, $\beta$ is the ratio of the electron velocity to the speed of light, and n and k are the wavelength dependent index of refraction and extinction coefficient of the dielectric medium, respectively. A sinusoidal variation of intensity with foil thickness is seen in the $\sin^2\left(\frac{\pi t}{\lambda_{ex}}\right)$ term. Equation (1) has been shown to apply only in the neighborhood of the plasma wavelength.[10]

### B. Transition Radiation

The theory of the emission of optical photons when a charged particle crosses the boundary between two dielectric media was first formulated by Frank and Ginzburg. This theory has been generalized

---

[9] Ferrell, loc. cit.

[10] Ritchie and Eldridge, loc. cit.

recently to include the wave properties of the incident charged particle by Ritchie and Eldridge.[11] The intensity of photons emitted per unit solid angle in the direction $\theta$ with respect to the incident electron direction, per unit wavelength interval at the wavelength $\lambda$ by a foil of thickness t is found to be

$$E(\theta,t,\lambda,\beta) = \frac{2e^2\beta^2}{\pi\lambda^2}\mu^2(1-\mu^2)\ |D|^2 \tag{2}$$

where

$$|D|^2 = \frac{1}{|\Delta|^2}\left|\left[\frac{\beta\sigma+\epsilon}{1-\beta^2\mu^2} - \frac{1}{1-\beta\sigma}\right](\mu\epsilon+\sigma)e^{-it\sigma} + \left[\frac{\beta\sigma-\epsilon}{1-\beta^2\mu^2} + \frac{1}{1+\beta\sigma}\right](\mu\epsilon-\sigma)e^{it\sigma}\right.$$

$$\left. - 2\sigma\left[\frac{\epsilon}{1-\beta\mu} - \frac{1+\beta\epsilon\mu}{1-\beta^2\sigma^2}\right]e^{-it/\beta}\right|^2,$$

$\Delta = (\mu\epsilon - \sigma)^2\ e^{it\sigma} - (\mu\epsilon + \sigma)^2\ e^{-it\sigma}$,

$\epsilon$ = the complex dielectric constant,

$\sigma = (\epsilon - 1 + \mu^2)^{1/2}$, and

$\mu = \cos\theta$.

A digital computer code for the IBM-7090 has been written by Ritchie and Eldridge to evaluate Equation (1) for a general dielectric constant having both a real and imaginary part. The optical data on

---

[11] Ritchie and Eldridge, loc. cit.

Au of R. Philip[12] were used in evaluating the theory and the spectral distributions were obtained for foil thicknesses of 340 Å and 530 Å. The results are shown in Figures 12 through 20 and will be discussed later with the experimental data.

## C. Bremsstrahlung

Another source of optical photons from electron irradiated solids is bremsstrahlung. Although emission from isolated atoms has been investigated theoretically, calculations on bremsstrahlung production in solids have not been carried out. Gluckstern, Hull, and Breit[13] give the spectral and angular distributions of photons averaged over all possible deflections of the electron. The differential cross section for bremsstrahlung production for photon energies small compared to the electron energy, and with photons polarized parallel to the plane of incidence, is

$$d\sigma_{\parallel} = Z^2 \left[ \frac{e^2}{\hbar c} \right] \left[ \frac{e^2}{m_o c^2} \right] \frac{(1-\beta^2)}{\beta^2} \frac{dk}{k} \frac{(\cos\theta - \beta)^2}{(1-\beta\cos\theta)^4} \times \sin\theta \, d\theta$$

$$\times \left\{ \ln \frac{(m_o c^2)^2 \beta^2}{(1-\beta^2)\left(k^2 \left[ \frac{1-\beta\cos\theta}{\beta} \right]^2 + \frac{Z^{2/3} (m_o c^2)^2}{(108)^2} \right)} + 0_{\parallel}(1) \right\} . \tag{3}$$

---

[12] R. Philip, Opt. Acta 7, 47 (1960).

[13] Gluckstern, Hull, and Breit, loc. cit.

For photons polarized perpendicular to this plane, the corresponding cross section is

$$d\sigma_{\perp} = Z^2 \left[ \frac{e^2}{\hbar c} \right] \left[ \frac{e^2}{m_o c^2} \right]^2 \frac{(1-\beta^2)}{\beta^2} \frac{dk}{k} \frac{1}{(1-\beta \cos \theta)^2} \times \sin \theta \, d\theta$$

$$\times \left\{ \ln \frac{(m_o c^2)^2 \beta^2}{(1-\beta^2) \left( k^2 \left[ \frac{1-\beta \cos \theta}{\beta} \right]^2 + \frac{Z^{2/3} (m_o c^2)^2}{(108)^2} \right)} + 0_{\perp} (1) \right\} \qquad (4)$$

where $\theta$ is the angle between the photon direction and the direction of the incident electron, Z is the atomic number of the foil material, k is the photon energy, and $0_{||}(1)$ and $0_{\perp}(1)$ are quantities of the order of unity. For the conditions encountered in the present experiment (photon energy $k < 20$ eV, $\beta > .2$, $z > 4$), the first term in the denominator of the logarithm is very small compared to the second term and the argument of the logarithm reduces to

$$\frac{(108)^2 \beta^2}{Z^{2/3} (1 - \beta)^2} .$$

For comparison with experiment the photon intensity per unit wave length per unit solid angle may be obtained from Equation (3),

$$E_{||}(\theta,t,\lambda,\beta) = NZ^2te^2 \left[ \frac{e^2}{m_o c^2} \right]^2 \frac{(1-\beta^2)}{\beta^2} \frac{1}{\lambda^2} \frac{(\cos\theta - \beta)^2}{(1-\beta\cos\theta)^4}$$

$$\times \left\{ \ln \frac{(108)^2 \beta^2}{Z^{2/3} (1-\beta^2)} + 0_{||} (1) \right\} \tag{5}$$

where N is the atomic density, $\lambda$ is the wave length in centimeters, and $E_{||}$ represents the photon intensity polarized parallel to the plane of incidence. The photon intensity per unit wave length per unit solid angle for photons polarized perpendicular to this plane may be obtained by multiplying Equation (5) by the ratio of the perpendicular bremsstrahlung component to the parallel bremsstrahlung component,

$$\left[ \frac{1-\beta\cos\theta}{\cos\theta - \beta} \right]^2 . \tag{6}$$

# III. APPARATUS

## A. Introduction and General Description

The apparatus consisted primarily of an electron gun, a linear accelerator, an irradiation chamber which housed the foil being irradiated and the Faraday cup, a scanning monochromator, a polarizer, a light detector, vacuum pumps, and the necessary voltage supplies and current measuring instruments (see Figure 1).

Electrons were accelerated from 25 keV to 120 keV with the beam being focused by adjustment of the electron gun supply controls and by two large degaussing coils located in horizontal and vertical planes near the electron beam. The coils also served to compensate for the earth's magnetic field and other stray magnetic fields in the laboratory. The spectrometer was positioned to receive light which was emitted from the foil at a 30° angle to the foil normal. Spectra were obtained with two orientations of the polarizer over the spectral region.

## B. Accelerator

The main body of the electron accelerator consisted of six accelerating electrodes separated by ceramic insulators. The electrodes were connected electrically by 50-meg resistors to insure equal accelerating potentials between one electrode and the next. High voltage for the accelerator was provided by a Sorensen and Company model 2120-5 R and D, dc, 120-kV, 5-ma, high voltage supply. Used in conjunction with the high voltage supply was a Sorensen L2, low ripple filter and a Sorensen

UNCLASSIFIED
ORNL-LR-DWG. 77665

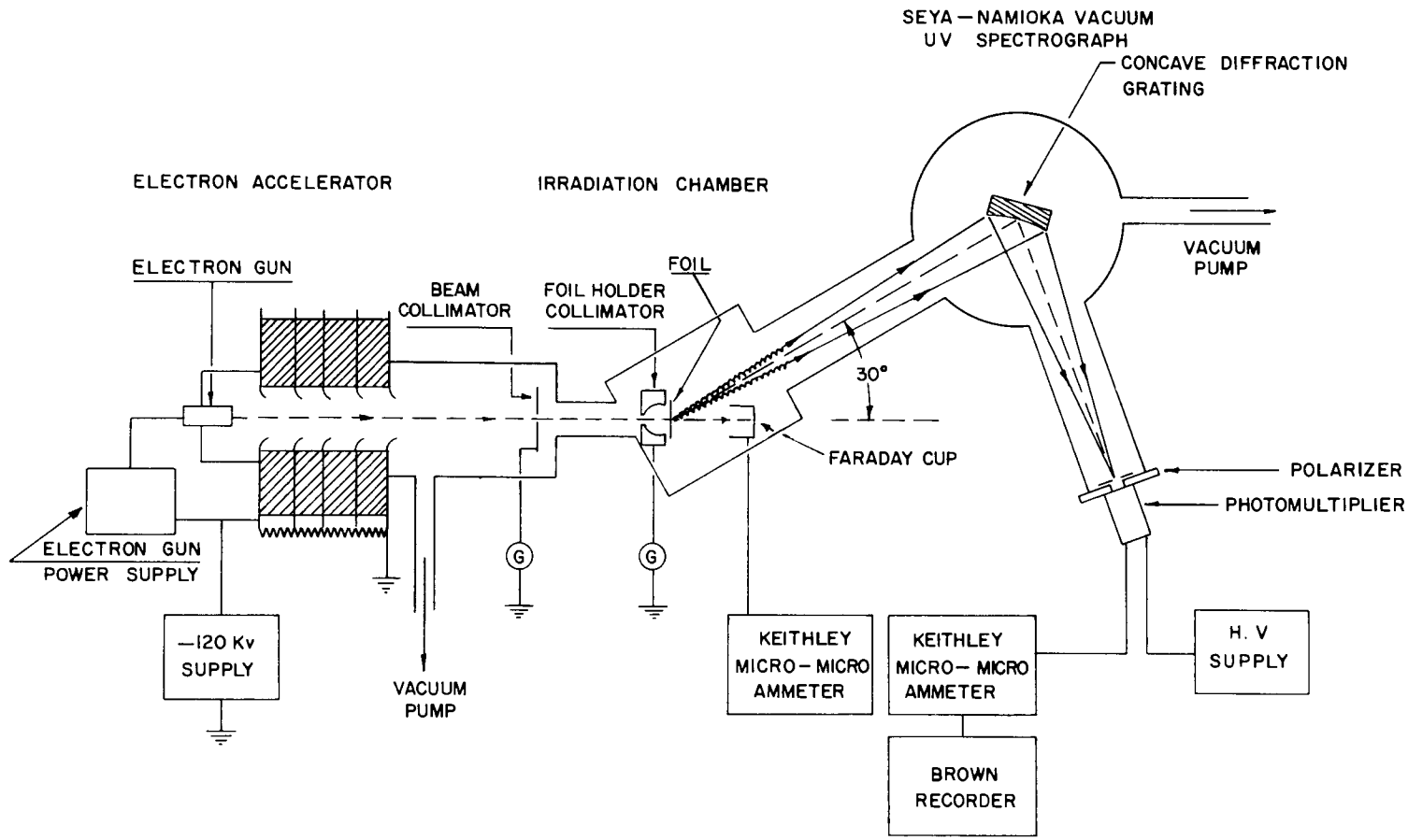


Fig. 1.—Schematic diagram of accelerator, irradiation chamber, and spectrometer.

2000 S line voltage regulator.

An oil-diffusion pump backed by a rotary forepump was connected to the accelerator to evacuate the internal system to operating pressures of 1-2 $\times 10^{-6}$ mm Hg. The accelerator was separated from the irradiation chamber by a Circle-Seal valve to facilitate changing of foils without letting the accelerator vacuum down to atmospheric pressure.

A small collimator insulated from the accelerator and connected electrically to a galvanometer was located in the accelerator near the irradiation chamber to aid in locating the electron beam.

The accelerator was located inside of an aluminum cage equipped with interlocks on the cage doors. The high voltage and electron gun supplies were shut off automatically when the cage doors were opened.

## C. Electron Gun

The electron gun consisted of a filament, a grid, an accelerating anode and a focusing anode. The filament was obtained from a Westinghouse 1709, 5-V light bulb which has a linear filament. The filament was coated with an emission coating obtained from the Kulite Tungsten Company, Ridgefield, New Jersey. The emission coating enhanced the electron emission and lifetime of the filament. Focusing of the electron beam was accomplished by adjusting the anode voltage, the grid voltage, and the filament current. The gun assembly was sealed in the accelerator with O-rings and by a small O-ring sealed flap valve which permitted re-coating of the filament without admitting air to the rest of the vacuum system.

The electron gun supply was the same as that used by Frank *et al.*[14] except for the addition of a very fine control to vary the filament current.

## D. Irradiation Chamber

The irradiation chamber made from a brass block was the same as used by Frank *et al.*[14] except for one minor modification. The foil holder was redesigned to allow two foils to be mounted at the same time. The two foils were mounted at right angles to each other to insure that only one would be irradiated at a time. The foil holder could be raised or lowered to permit the beam to strike either foil. The foil holder had a 2-mm diameter collimator and was so designed that light produced at the collimator could not be detected by the photomultiplier. The irradiation chamber also housed the Faraday cup used to collect the beam current. The chamber was connected to the monochromator by a metal flange with an O-ring seal and to the accelerator by a bellows attachment with a flange and O-ring seal. A lucite plate on top of the chamber permitted visual observation of the beam as it impinged on the target.

## E. Spectrometer

A Jarrell-Ash model 78-650 Seya-Namioka vacuum scanning spectrometer was used for spectral measurements. An important feature of the Seya is that with proper adjustment of the angle made by the entrance

---

[14] A. L. Frank *et al.*, Oak Ridge National Laboratory Report, ORNL-3114, 1962.

slit, the grating, and the exit slits and the grating, only a negligible change in focus is noted over a fairly broad spectral region. This permitted rapid spectral scans of a 4000- or 5000-Å region. The spectrometer was focused visually by adjustment of the grating tilt and the spectrometer arm length through the use of the Foucault knife-edge test. The grating was rotated at speeds varying from 10 Å per min up to 5000 Å per min, although usually the speed was 1000 Å per min. The combination of entrance and exit slits gave a resolution of about 40 Å. The spectrometer was evacuated to pressures of about $10^{-6}$ mm Hg by an oil diffusion pump, forepump, and liquid nitrogen cold trap.

The grating used in the spectrometer was a Bausch and Lomb .5-meter concave replica grating ruled with 15,000 lines per in. and blazed for 3500 Å. The ruled surface of the grating was 30 X 50 mm and was coated with MgF over aluminum. The transmission of the grating was measured for ordinary and polarized light with a grating calibrator described elsewhere over a spectral region from 1000 Å to 6600 Å.

An EMI No. 6256B photomultiplier with a 1-cm diameter photocathode was used as the light detector. Photomultiplier currents were measured with a Keithley model 410 micro-microammeter fed into a Minneapolis-Honeywell Brown recorder. The photomultiplier was operated at 1000 V supplied by a NJE Corporation model S-325-D249 high voltage supply.

## F. Polarizer

The polarizer used in the experiment was a Glan prism which transmits into the ultraviolet to about 2100 Å. The polarizer was

centered in a steel plate and rotated manually by a knob external to the vacuum system. The polarizer was located in the light path between the exit slit of the spectrometer and the photomultiplier. Transmission curves were obtained with the polarizer set for light polarized in the plane of incidence and perpendicular to the plane of incidence.

## G. Current Measuring Instruments

Both the beam current and the photomultiplier current were measured with Keithley model 410 micro-microammeters. Typical photomultiplier currents were in the $10^{-4}$ to $10^{-5}$ μa range. The amplified photomultiplier current was recorded by a Minneapolis-Honeywell Brown recorder, equiped with a side marking pen so that either 20-, 100-, or 200-Å intervals could be marked on the recording chart. The beam collimator in the accelerator and the foil holder were connected to Leeds and Northrup galvanometers to aid in locating and focusing the electron beam. A zero deflection on the beam collimator galvanometer indicated that the beam was passing through the collimator while a minimum deflection on the foil holder galvanometer indicated that the beam was passing through the foil holder collimator.

## H. Vacuum System

Two oil-diffusion pumps, Consolidated Electrodynamics Corporation, type MCF-300, backed by Welch Duo-Seal rotary forepumps were used to evacuate the system. One diffusion pump was connected by a large valve to the spectrometer chamber while the other diffusion pump was connected by another large valve located at the accelerator. Both

diffusion pumps were isolated from the vacuum system by liquid-nitrogen cold traps located between the diffusion pumps and the large valves. Normal operating pressure was $10^{-6}$ mm Hg.

# IV. THIN FOIL PREPARATION AND THICKNESS DETERMINATION

## A. Foil Preparation

The apparatus and techniques for foil preparation have been discussed quite thoroughly elsewhere,[15-17] and will be discussed only briefly here.

The foils are prepared by the vacuum evaporation method. The evaporation is performed under a Bell jar at reduced pressures of no greater than $10^{-5}$ mm Hg. A known mass of metal is evaporated from a "boat" onto a clean glass microscope slide. The thickness t of the foil being prepared is approximated from the inverse square law,

$$t = \frac{m}{2\pi r^2 \rho} \tag{7}$$

where m is the mass of the metal being evaporated, r is the perpendicular distance from the slide to the "boat", and $\rho$ is the density of the metal. Before the metal is evaporated, a "wetting agent" is deposited on the slide, also by vacuum evaporation. The choice of a wetting agent is determined by the metal being deposited.[17] Basically, the wetting agent must not alloy with the metal being deposited and it must be water soluble. If the wetting agent is water soluble, it is possible to

---

[15] L. Holland, Vacuum Deposition of Thin Films (John Wiley and Sons, Inc., New York, 1960).

[16] F. Kalil et al., Oak Ridge National Laboratory Report, ORNL-2731, 1959.

[17] P. L. Ziemer et al., Oak Ridge National Laboratory Report, ORNL-2775, 1959.

"float" off the vacuum deposited metallic film on water.

The slide was slowly immersed at an angle into a beaker of lukewarm, distilled water. As the wetting agent dissolved, the metallic film slowly floated off onto the surface of the water, being held up by the surface tension of the water. The floating off was aided somewhat by scratching the edge of the slide where the metal was deposited, thus enabling water to reach the wetting agent.

Once the metallic foil was separated from the microscope slide, it was mounted on a 5/8-in. diameter aluminum disc, .005 in. thick, with a 1/4-in. diameter hole in its center. Mounting the floating metallic film on the aluminum disc was accomplished by completely submerging the disc in the water and then, with the disc tilted at an angle to the surface of the water, slowly withdrawing the disc from the water and at the same time picking up the foil on the disc. When the metallic film was floated off in one piece, it was possible to salvage at most only three smooth mounted foils since whenever the disc was withdrawn from the water with the foil adhering to it, a certain amount of the area of the floating film was destroyed. Because the film was so thin, a slight disturbance of the water surface caused the film to break into tiny pieces. By scratching a 1-cm grid on the film after evaporation, it was possible to salvage up to ten foils from one microscope slide. This process also had the advantage of permitting only the desired number of squares to be floated off, and thus allowed the remainder of the film on the slide to be stored for later use.

B. Determination of Foil Thickness

Two methods were employed to determine the thickness of the gold foils used as targets. One used a modified commercial electrobalance and the other an optical interferometer.

1. Electrobalance method.—Foils of area 1 $cm^2$ were weighed on a modified Cahn Electrobalance, model M10, to determine the foil thickness in $\mu g/cm^2$. The modifications of the electrobalance and the weighing procedure were developed by Kalil *et al.*[18] and made possible the weighing of samples in the 1- to 100-$\mu$g range. A complete description of the apparatus, the modifications and the procedure are given in the publication by Kalil *et al.* The electrobalance was used also as a check on the uniformity of the thickness of a metallic deposit over the surface of a microscope slide. The results shown here are not conclusive due to the small number of samples, but are illustrative enough to show that the thickness of the metallic deposit across the slide does not vary significantly. This variation in thickness occurs since the deposit of the metal on the film more closely follows a $\cos^4$ distribution,

$$t = \frac{m \cos^4 \theta}{2\pi r^2 \rho} \tag{8}$$

rather than the approximation used as Equation (7). The angle $\theta$ is defined by a normal to the microscope slide and the direction of the molecules as they deposit on the slide. This equation indicates that the thickness of the metallic film on a microscope slide 7.5 cm long,

[18] Kalil *et al.*, *loc. cit.*

located 13.5 cm from the source, will be smaller at the ends when compared with the thickness at the center of the slide by a factor of 0.855.

Two microscope slides were located in the vacuum evaporating apparatus at distances of 12.5 and 25 cm from a source of 82.6 mg of silver. From Equation (7), the slide located at 12.5 cm was to have a film 800 Å thick at its center while the slide located at 25 cm was to have a film approximately 200 Å thick at its center. After evaporation the two slides were carefully scratched as shown in Figure 2 so that ten 1-$cm^2$ samples could be floated off and mounted on weighing pans to be used in the electrobalance.

Thirteen aluminum weighing pans approximately 1.6 $cm^2$ and 0.0127 cm thick were weighed without the 1-$cm^2$ silver sample. Pans Nos. 5, 11, and 13 were used to detect any change in the calibration of the electrobalance during the time required to weigh the ten samples. The ten samples were then mounted on the pans and will be referred to by number as shown in the schematic diagram. Samples 8 and 12 unfortunately were lost in the mounting process. The samples were allowed to dry completely before they were weighed. The calibration of the electrobalance did not change during the weighing of the samples. The results are shown in Table 1, where the thicknesses of the samples have been calculated with the assumption that the density of the evaporated foils is the same as the bulk density of the material. There is some doubt as to whether the density of the deposited film equals bulk density. An excellent discussion of the physical properties of thin films has been given

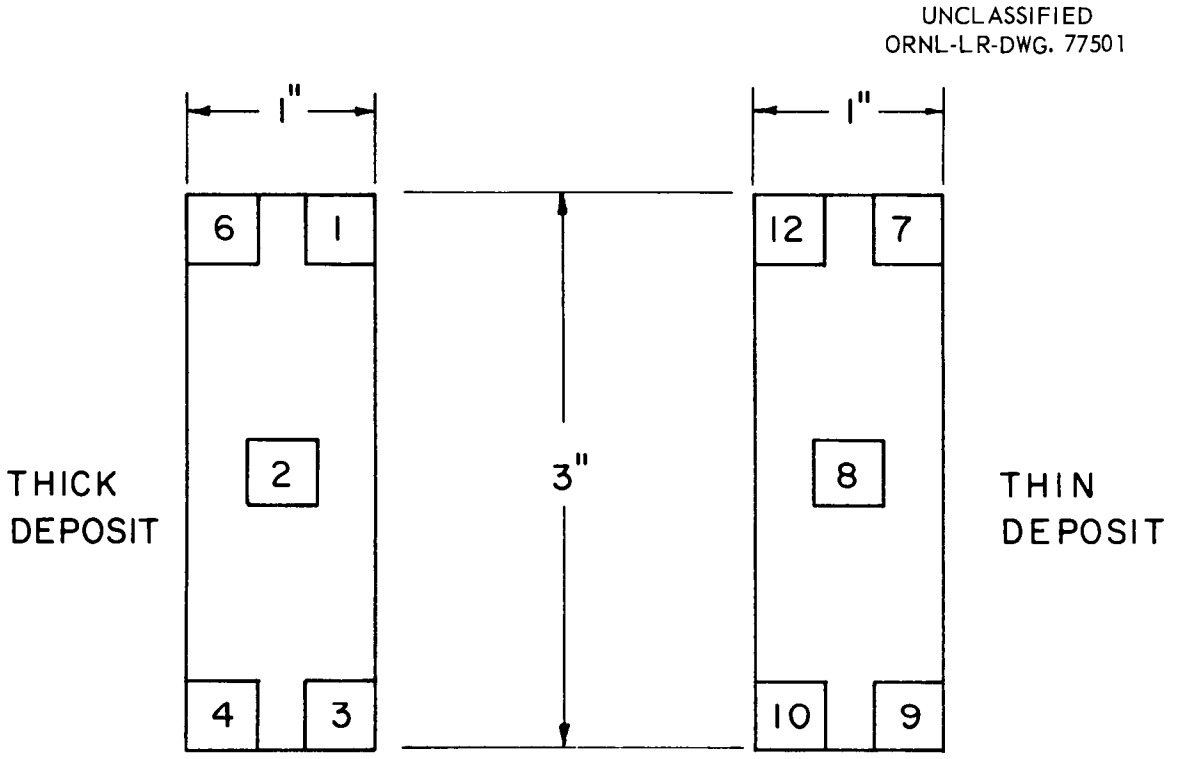


Fig. 2.—Schematic diagram of samples used to check variation in foil thickness.

recently by Neugebauer.[19]

TABLE 1

VARIATION OF FOIL THICKNESS AS A FUNCTION OF POSITION ON GLASS SLIDE

| Sample | Density Thickness ($\mu g/cm^2$) | Thickness in Å Using Bulk Density |
|---|---|---|
| 1 | 124 | 1190 |
| 2 | 159 | 1515 |
| 3 | 137 | 1305 |
| 4 | 144 | 1370 |
| 6 | 137 | 1305 |
| 7 | 32 | 305 |
| 9 | 34 | 324 |
| 10 | 34 | 324 |

The results show that the thickness of the deposited film does vary across the surface of the microscope slide, being thicker at the center in approximate agreement with the $\cos^4$ dependence of Equation (8). If the thickness of the film at the ends of the slide can be assumed to be the average of samples 1, 3, 4, and 6, then the ratio of this average to the thickness at the center for the slide with the thick deposit is 0.85 as compared with a theoretical value of 0.855 calculated from Equation (8).

The usual procedure in preparing an irradiation target was to mount a part of the film on an aluminum disc and then to collect another

[19] J. A. Neugebauer et al., Structure and Properties of Thin Films (John Wiley and Sons, Inc., New York, 1959).

small segment on a weighing pan to determine the thickness. The variation in thickness of the film over the surface of the microscope slide shows that the sample being weighed should be chosen so that its geometrical location with respect to the source was the same as the segment mounted on the aluminum disc.

2. Interferometric method.—The interferometric method of thickness determination eliminates any doubt about a probable change in the density of the bulk metal through evaporation and deposition. The theory for light emitted from metals contains the thickness of the metallic foils as one of the variables and the interferometric method gives this metric thickness directly as opposed to density thickness obtained with the electrobalance method.

The auxiliary optics, the interferometer, and microscope were optically aligned, as described by Tolansky,[20,21] and are shown schematically in Figure 3. A green mercury filter used with a mercury arc source permitted monochromatic light of wavelength 5461 Å to be incident on the interferometer. A convex lens, 5.2 cm in diameter, with a 22-cm focal length was placed in the light path at a distance of 22 cm from the mercury arc source so that the light incident to the interferometer was parallel. The half-silvered mirror makes a 45° angle with the optical axis of the auxiliary optics and thus light is incident normal to the interferometer. The interferometer consists of a glass

---

[20] S. Tolansky, An Introduction to Interferometry (Longmans, Green, and Co., London, 1955).

[21] S. Tolansky, Surface Microtopography (Interscience Publishers, New York, 1960).

UNCLASSIFIED
ORNL-LR-DWG. 77500

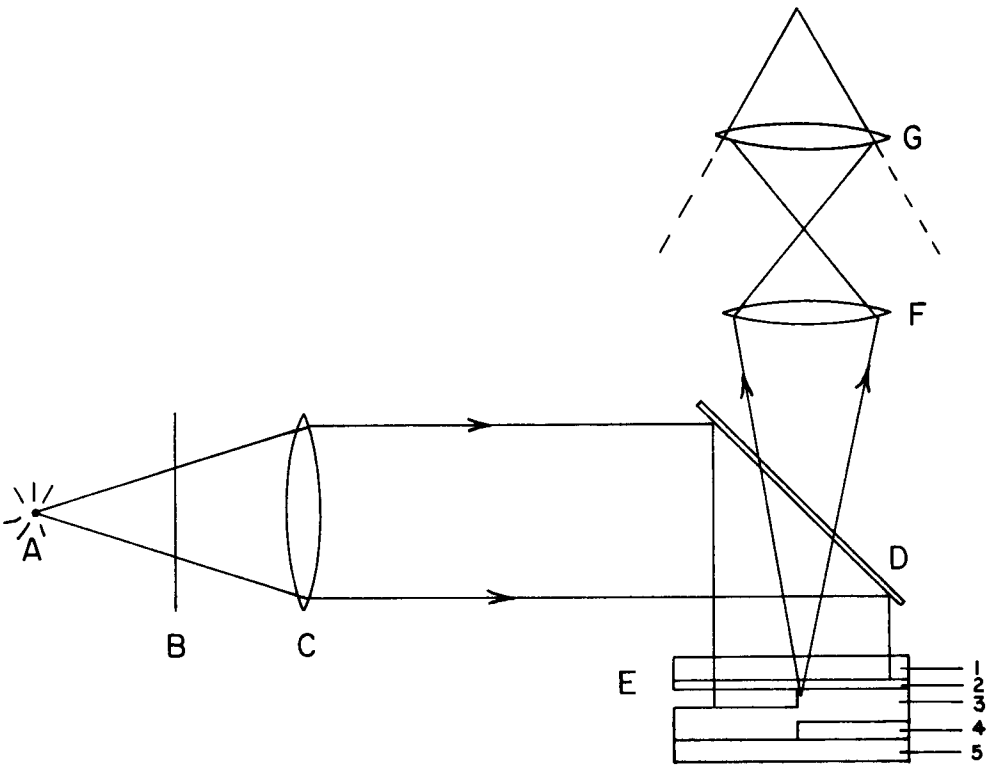


A. MERCURY ARC SOURCE
B. GREEN MERCURY FILTER
C. 22-cm FOCAL LENGTH LENS
D. HALF-SILVERED MIRROR
E. INTERFEROMETER
F. G. MICROSCOPE

1. OPTICAL FLAT
2. SILVER DEPOSIT ON OPTICAL FLAT
3. SILVER DEPOSIT ON THIN FILM AND SLIDE
4. THIN FILM
5. MICROSCOPE SLIDE

Fig. 3.—Schematic diagram of optical interferometer.

microscope slide which had a small fragment of a thin film on it. A thick deposit of silver was then evaporated onto the slide completely covering and at the same time contouring the thin film fragment. This resulted in a step profile on the slide. An optical flat with a half-silvered thickness of silver on it was then placed in a simple jig which had three screws that served to adjust the wedge between the slide and the flat, thus bringing the fringes into focus in the microscope. Where the step occurs due to the thin film on the slide, a small shift is observed in the fringe pattern. This is shown in Figure 4 and represents a film thickness of 425 Å. The film thickness T is calculated from the relation

$$T = f \frac{\lambda}{2}$$

where f is the fractional shift or displacement of the fringe at the step and $\lambda$ is the wavelength of the incident monochromatic light.

Two types of microscopes were used to determine the fractional fringe shift, f. One was a Bausch and Lomb model BVB-63 Stereozoom variable power model. Measurement of $\Delta n$ was made possible through the use of a micrometer eyepiece. Several measurements on various fringe patterns showed that the determination of the film thickness was reproducible to within about $\pm$ 25 Å for films whose thicknesses were about 900 Å or greater. The magnification of this instrument was too low to give satisfactory results for films of thickness 500 Å or less. The other microscope used was a modified Leitz Panphot photomicrograph apparatus. The built-in light sources of the Leitz Panphot were removed from the instrument so that the optical interferometer shown in

UNCLASSIFIED
PHOTO 61522

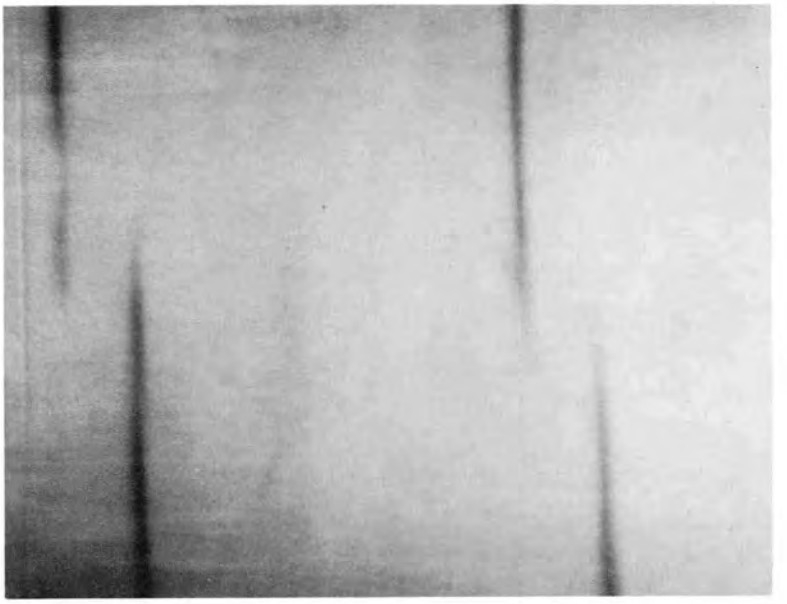

Fig. 4.—Photograph of fringe shift for a 425-Å thick foil.

Figure 3 could be used. Also, the film holder was removed and replaced by a Polaroid camera from which the lenses had been removed. The Polaroid camera made it possible to develop the film taken of a fringe pattern immediately after exposure and thus assure quickly that correct focusing had been achieved. Once a photograph of the fringe pattern had been obtained, the fringe shift could be measured to within $\pm$ 10 Å. The capability to measure the film thickness with a photograph depended on bringing the fringes in sharp focus and this required very precise lenses such as those supplied with the Leitz Panphot.

# V. CALIBRATION OF APPARATUS

## A. Calibration with a Standard Light Source

The calibration of the apparatus in the visible and near ultraviolet spectral regions is relatively simple. From 2500 Å to 7000 Å a standard lamp of known spectral radiance was used as a light source. By measuring the output of the standard lamp as a photomultiplier current in amps and employing the same geometry as used in the determination of the light produced by electron bombardment of thin foils, the calculation of the spectral radiance $P_f(\lambda)$ of the irradiated thin foil was given by

$$P_f(\lambda) = \left[\frac{P_s(\lambda)}{I_s(\lambda)}\right] \frac{I_f(\lambda)}{I_e} \tag{9}$$

where $I_f(\lambda)$ is the photomultiplier current for light from a thin foil bombarded by an electron beam current $I_e$, $P_s(\lambda)$ is the known spectral radiance of a standard light source, and $I_s(\lambda)$ is the photomultiplier current for light from the standard light source at the foil position with reference to the spectrometer.

The standard light source was a tungsten ribbon filament lamp, G.E. type 30A/T24/3, supplied by the National Bureau of Standards which had been previously calibrated against a black body. The maximum uncertainty in the NBS calibrations was estimated to range from about 8% at the shortest wavelength to about 3% at the longest wavelength.[22] The

[22] R. Stair *et al.*, J. Research Natl. Bur. Standards 64A, 291 (1960).

auxiliary optics employed in the calibration were the same as shown by Stair *et al.*[23] so that a one-to-one magnification of the tungsten filament was focused on the entrance slit of the monochromator. Slits of the same size as used in the actual experiment were employed as well as the same grating, photomultiplier, and micro-microammeter. During the calibration the grating was completely filled with light, as was true also during the experiment. Two corrections were necessary to determine the ratio of the input to the output of the standard lamp. The use of a plane mirror and a spherical mirror in the auxiliary optics meant that some light was lost at the two reflecting surfaces. Since both mirrors were aluminized at the same time, their reflectivity was assumed to be the same. The reflectivity of the plane mirror was experimentally determined as a function of wavelength, and the square of the reflectivity was used to correct for the light lost at the mirrors. The second correction was required because the output of the standard lamp was so intense as to require the operation of the photomultiplier at a reduced voltage of 600 V rather than the 1000 V normally used in the experiment. The ratio $C_e(\lambda) = \left[\frac{P_s(\lambda)}{I_s(\lambda)}\right]$ required to convert photomultiplier current to photon intensity at the gold foil is shown in Figure 5 and is in units of electron volts per steradian per centimeter of wavelength per electron.

## B. Calibration in the Far Ultraviolet

The unavailability of a light source of known spectral radiance in the region below 2500 Å makes the calibration of the apparatus in

[23] *Ibid.*

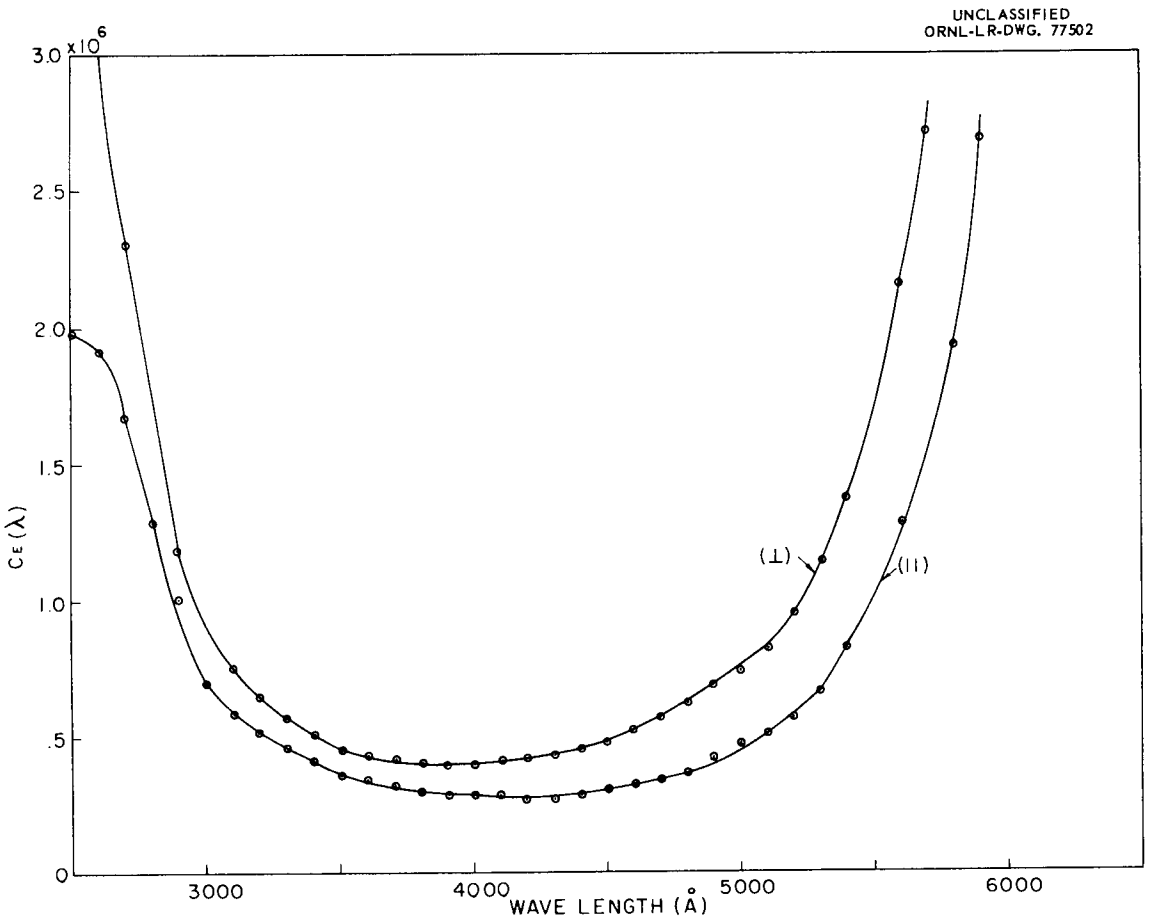


Fig. 5.—Correction factor for spectral response of spectrometer.

this region quite difficult. The photomultiplier current $I_{ph}$ is a function of $\Omega$, the solid angle subtended by the grating, P, the spectral response of the photomultiplier, and T, the transmission of the spectrometer. The relationship between $I_{ph}$ and the intensity of the light emitted by the foil I is

$$I_{ph}(\lambda) = I(\lambda)\ P(\lambda)\ \Omega(\lambda)\ T(\lambda). \tag{10}$$

The accurate determination of $I(\lambda)$ in the far ultraviolet is thus limited by the accuracy of measurements of $P(\lambda)$, $\Omega(\lambda)$, and $T(\lambda)$.

1. Spectral response of the photomultiplier, $P(\lambda)$.—There are two ways in which $P(\lambda)$ can be determined. In the first the light emitted from an uncalibrated ultraviolet source is determined using a calibrated black body detector such as a thermopile. This same source can then be investigated with the photomultiplier to determine the response function $P(\lambda)$.

The second method, and the one used here, is to use a light converter whose quantum efficiency as a function of wavelength is known. The fluorescent material sodium salicylate has been found to have a constant quantum efficiency from 500 Å to 3000 Å,[24] and thus the photomultiplier response to have a plateau over this spectral region. The absolute response was determined in the overlap region from 2500 Å to 3000 Å, where data from the standard lamp source were available.

---

[24] K. Watanabe and E. C. Y. Inn, J. Opt. Soc. Am. 43, 32 (1953).

2. Solid angle subtended by the grating, $\Omega(\lambda)$.—In scanning the spectrum in the first order from the central image to 7000 Å, the grating rotates through an angle of about 15°. The effective area of the grating A is calculated from the relation,

$$A = A_o \cos \alpha \tag{11}$$

where $A_o$ is the area of the ruled portion of the grating and $\alpha$ is the angle made by the normal to the grating and the direction of the incident light. The angle $\alpha$ thus becomes a function of the wavelength of light dispersed to the exit slit of the spectrometer and is calculated from the grating equation,

$$n\lambda = d(\sin \beta - \sin \alpha) \tag{12}$$

where d is the grating constant, and $\alpha$ and $\beta$ are the angles made by the grating normal with the entrance and exit slits of the spectrometer, respectively. The solid angle correction is determined from the relation,

$$\Omega(\lambda) = \frac{A_o \cos \alpha}{R^2} \tag{13}$$

where R is the distance from the grating to the light source. In scanning the spectrom from 0 to 6200 Å the solid angle varies from $0.819\ A_o R^{-2}$ to $0.927\ A_o R^{-2}$. The solid angle correction is required if the ruled portion of the grating is the limiting aperture in the light path. In order to eliminate this problem, a baffle with the minimum effective grating dimensions was placed in the light path. The solid

angle then remained constant at $0.819\ A_o R^{-2}$ when the grating was rotated.

3. Transmission of the spectrometer, $T(\lambda)$.—The total transmission of the spectrometer, $T(\lambda)$, is the product of the grating efficiency, $T_o(\lambda)$, and a geometrical factor due to the image enlargement, $G(\lambda)$, or

$$T(\lambda) = T_o(\lambda)\ G(\lambda). \tag{14}$$

The efficiency of the grating used as the light dispersing element in the spectrometer is defined here as the ratio of the light reflected from the grating to the light incident on the grating.

The longitudinal magnification of the entrance slit at the exit slit of the spectrometer is due to astigmatism which results from the use of a spherical concave diffraction grating at non-normal incidence. The astigmatism has been treated by T. Namioka for spherical concave diffraction gratings.[25] Using the Seya-Namioka geometry for a 50-cm radius of curvature grating ruled with 15,000 lines per in., Namioka showed that for grating rulings 30 mm long, the image should be 20 mm long, both values being true only for a point source. For a line source 12 mm long as used here, this astigmatism would result in an image 32 mm long for the central image. Little error is introduced if the assumption is made that the astigmatism is constant for a particular grating and independent of wavelength. Thus, Equation (14) may be rewritten as

$$T(\lambda) = T_o(\lambda) G. \tag{15}$$

---

[25] T. Namioka, J. Opt. Soc. Am. 51, 13 (1961).

The height of the exit slit in the monochromator is 12 mm as compared with the calculated 32 mm for the image. This means that a large percentage of the light reflected by the grating is not detected by the photomultiplier. If the image were rectangular in shape, there would be little difficulty in determining G. However, the image is crescent shaped and thus equal intervals along the length of the image do not represent intervals of equal intensity. A simple experiment was devised to measure the length of the image formed at the exit slit as well as to determine the per cent of the reflected light detected by the photomultiplier. A light source, an entrance slit 12 mm long, a grating with rulings 30 mm in length and a photomultiplier were arranged in the Seya-Namioka geometry. The photomultiplier was attached to a micrometer microscope so that it could be raised and lowered in accurate intervals. The photocathode of the photomultiplier was masked to give a horizontal slit about 5 mm wide by 1 mm high. This helped to reduce any error involved in the experiment which would be introduced due to the non-uniformity of the response of the photomultiplier across the area of the photocathode. With a longitudinally magnified image of the entrance slit focused on the 5 x 1-mm horizontal slit, the photomultiplier was raised in 1-mm intervals and the intensity of the light was measured and recorded for each interval. The total number of intervals for which any light could be detected then gave the height of the image. The ratio of the sum of the intensities of a 12-interval central section of the image to the sum of the intensities of all the intervals was the fraction of the light reflected from the grating which was detected by the photo-

multiplier. The results of the experiment showed that the image was 29 mm long and that only 56.7% of the reflected light was detected by the photomultiplier. The correction factor G was then 1 divided by 0.567 or 1.764, for 12-mm long entrance and exit slits.

Often the transmission of a grating is assumed to be flat or equal to the reflectivity of the metallic surface of the grating. Measurements of the efficiencies of several spherical concave diffraction gratings showed that the absolute transmission was far from flat and was always less than the reflectivity of the metal which coated the grating.

4. The grating calibrator.—A grating calibrator was designed[26] and constructed to determine the absolute efficiency of concave diffraction gratings. The grating calibrator was unique in several ways. It measured the absolute efficiency of the grating in a manner which was independent of the response of the light detector. In addition, as the calibrator has as its only reflecting surface the grating being calibrated, it was itself a usable scanning vacuum spectrometer. Figure 6 shows the calibrator used in conjunction with the Seya monochromator which served as a monochromatic light source, and Figure 7 is a schematic diagram of the assembly.

The grating calibrator consists of a vacuum-tight chamber constructed of 5/8-in. and 3/4-in. aluminum plate with external dimensions of 20 X 26 X 10 in. It contains an access portal located in the top for the light detector, an access portal located on one side for the grating, another portal for the light beam and vacuum-tight electrical connectors

[26] D. C. Hammer *et al.* (to be published).

UNCLASSIFIED
PHOTO 56900

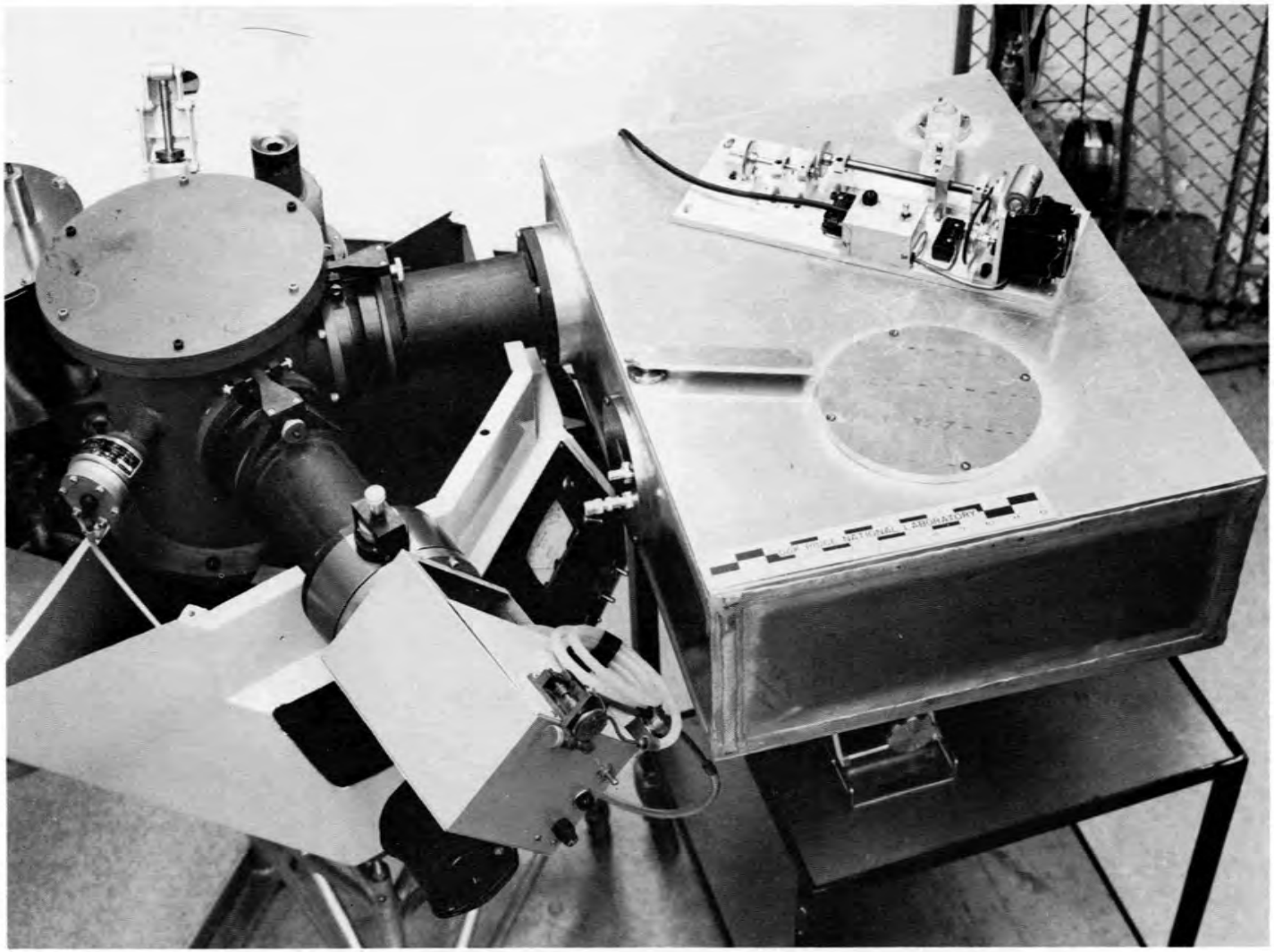

Fig. 6.—Photograph of ultraviolet spectrometer and grating calibrator.

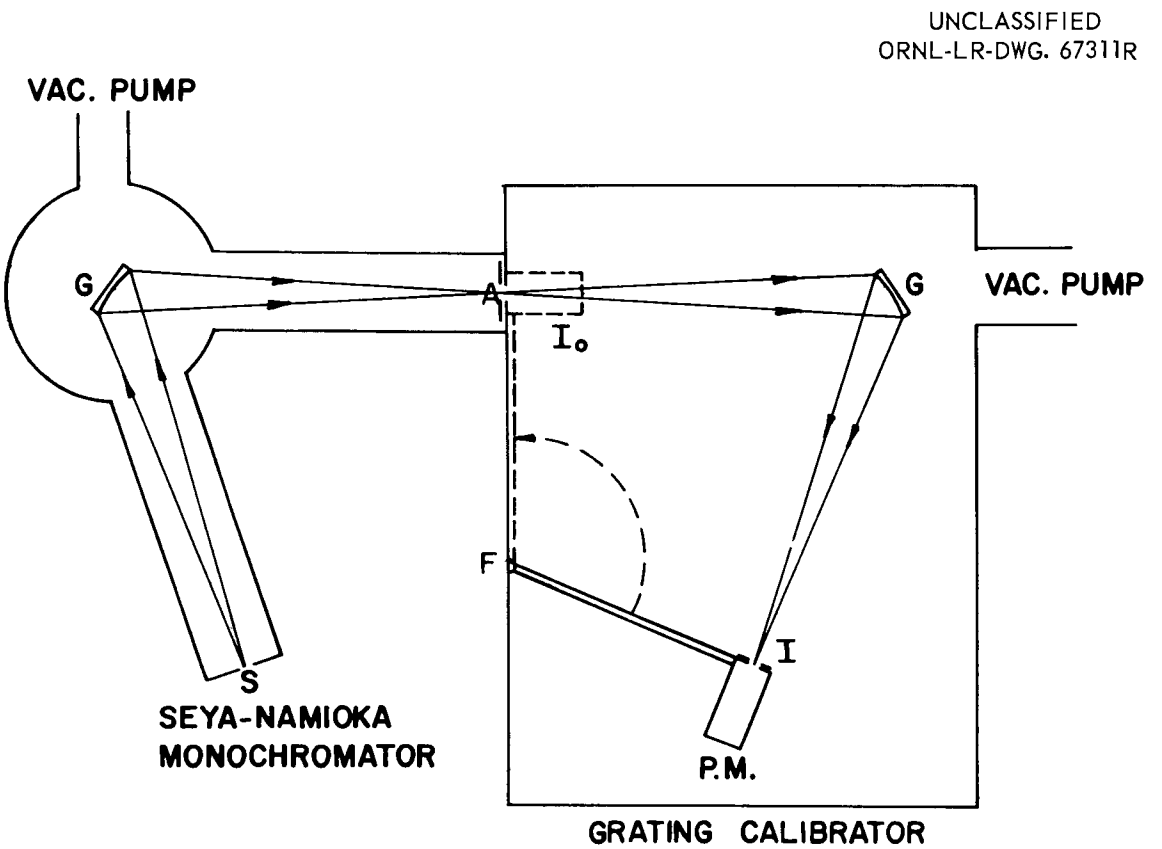


Fig. 7.—Schematic diagram of ultraviolet spectrometer and grating calibrator.

for the high voltage and signal leads to the light detector. The light detector is attached to a movable arm which can be used in two positions to measure the light incident on and reflected from the grating being calibrated. Rotation of this arm is accomplished with an arm external to the vacuum system but in the same shaft. The internal arm also carries a slit assembly. The grating being calibrated is attached to a table located inside the chamber and which is also rotated by an external arm. Rotation of the external grating arm can be done manually or by a motor-driven gear assembly with a wavelength indicator. The beam entrance portal contained a mount for a slit assembly and a slit.

The calibrator was designed according to the Seya-Namioka geometry for a 50-cm radius of curvature concave diffraction grating. The entrance slit to the calibrator was 10 mm long. The slit directly in front of the photomultiplier was 12 mm long and 2 mm wide. The photomultiplier was an EMI No. 6256-B with a 10-mm photocathode coated with sodium salicylate. Photomultiplier currents were measured with a Keithley model 410 micro-microammeter fed into a Minneapolis-Honeywell Brown recorder. With proper alignment of the optical path, all of the light entering the calibrator at the entrance slit was detected by the photomultiplier in the "$I_o$" or entrance slit position. The photomultiplier current $I_o(\lambda)$ was

$$I_o(\lambda) = N(\lambda)\ P(\lambda) \tag{16}$$

where $N(\lambda)$ is the amount of light entering the calibrator, and $P(\lambda)$ is the response of the photomultiplier. The photomultiplier current $I(\lambda)$

in the "I" or exit slit position of the calibrator was

$$I(\lambda) = \frac{N(\lambda)\ P(\lambda)\ T(\lambda)}{G} \tag{17}$$

where $N(\lambda)$ and $P(\lambda)$ have been previously defined, $T(\lambda)$ is the absolute transmission of the grating, and $1/G$ is the fraction of light lost due to optical aberration. The apparent transmission of the grating $T_o(\lambda)$ was the ratio of the photomultiplier currents,

$$T_o(\lambda) = \frac{I(\lambda)}{I_o(\lambda)} = \frac{T(\lambda)}{G}\ , \tag{18}$$

and the absolute efficiency of the grating (i.e., if all of the light reflected by the grating was collected by the photomultiplier) was

$$T(\lambda) = T_o(\lambda)\,G = \frac{I(\lambda)}{I_o(\lambda)}\,G. \tag{19}$$

In performing the calibration of a grating blazed at 3500 Å, the image was not enlarged to 30 mm as predicted by Namioka for a 10-mm entrance slit and 30-mm long grating rulings because the angle of divergence of the beam of light entering the calibrator was kept small to insure that no light was lost due to overfilling the grating. In order to determine the fraction of light detected by the photomultiplier in the "I" position, a photomultiplier with a 25-mm photocathode was placed in the "I" position in the grating calibrator. Circular apertures of 6, 8, 10, and

12 mm were then placed over the photocathode and the light detected for the central image was measured and recorded. A measurement taken with the photomultiplier unshielded indicated the total amount of light received by the photomultiplier. The results of this experiment showed that 86% of the light reflected by the grating was detected by the 10-mm diameter photocathode. Thus the value of G was 1.163 for the grating blazed for 3500 Å when used with a photomultiplier having a 10-mm photocathode. The value of G was found to be approximately constant over all wavelengths from the central image to 6000 Å. The absolute efficiency $T(\lambda)$ of the grating blazed at 3500 Å was then calculated from the measured photomultiplier currents according to the relation,

$$T(\lambda) = \frac{I(\lambda)\ (1.163)}{I_o(\lambda)} \tag{20}$$

Figure 8 shows the efficiency $T(\lambda)$ as a function of wavelength of a grating blazed for 3500 Å and ruled with 15,000 lines per in. The curve represented by crosses and open circles was determined with unpolarized light on the blazed side of the central image. The crosses represent data taken with an air discharge source while the open circles were obtained using a tungsten filament light source. The triangles represent data taken with light plane polarized parallel to the grating rulings on the blazed side of the central image while the squares represent data obtained with light plane polarized perpendicular to the grating rulings and also on the blazed side of the central image. The bottom curve shows a plot of the efficiency for unpolarized light on the

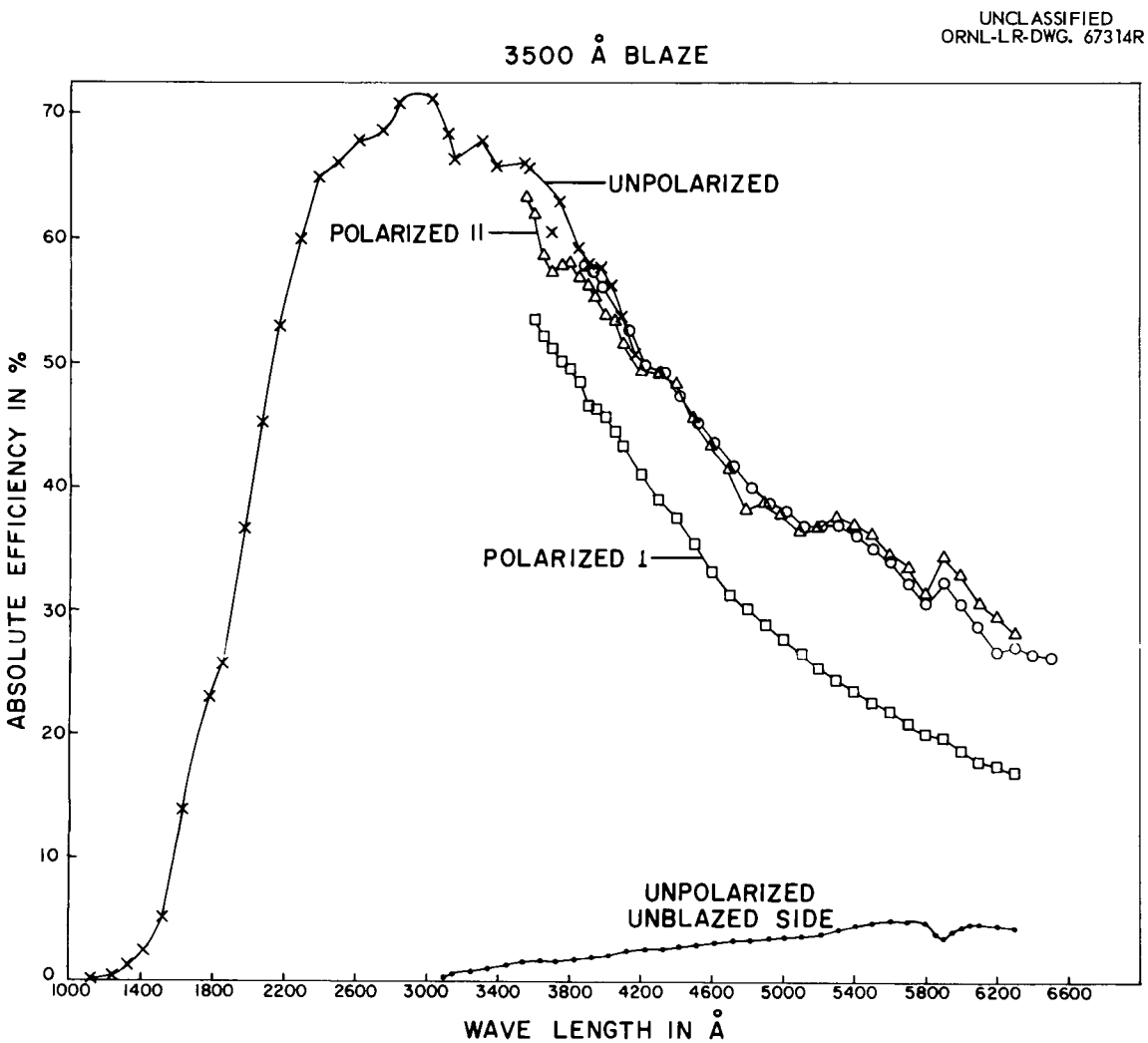


Fig. 8.—Absolute efficiency of 3500-Å blaze grating as a function of wavelength.

unblazed side of the central image. All four curves represent the efficiency in the first order.

It should be noted here that the blaze stated by the manufacturer is intended for light incident normal to the grating. As this is not the case with the Seya-Namioka spectrometer, one should not expect the experimentally determined efficiency to be a maximum at the same wavelength as that indicated by the manufacturer. With the Seya-Namioka geometry, the angle made by the entrance and exit slits is approximately 70°. This means that, according to theory, the grating should be most efficient at 3500 Å cos 35° or 2850 Å. This agrees quite well with the experimentally determined value of 2940 Å.

Figure 9 is a plot of the efficiency of a grating supposedly blazed for 6000 Å and ruled with 15,000 lines per in. The two curves represent the efficiency on each side of the central image in first order. The upper curve represents points taken on the blazed side (the side of the grating which should show the higher efficiency) and the lower curve shows the efficiency on the opposite side of the central image. This grating is not blazed for 6000 Å as stated by the manufacturer and the efficiencies are about the same on both sides of the central image.

Figure 10 shows the efficiency for a grating supposedly blazed for 1100 Å and ruled with 30,000 lines per in. The efficiency is somewhat difficult to determine at short wavelengths since the reflectivity of the surface of the grating falls off rather rapidly. This is a rather poor grating as it reflects no more than 10% of the incident light.

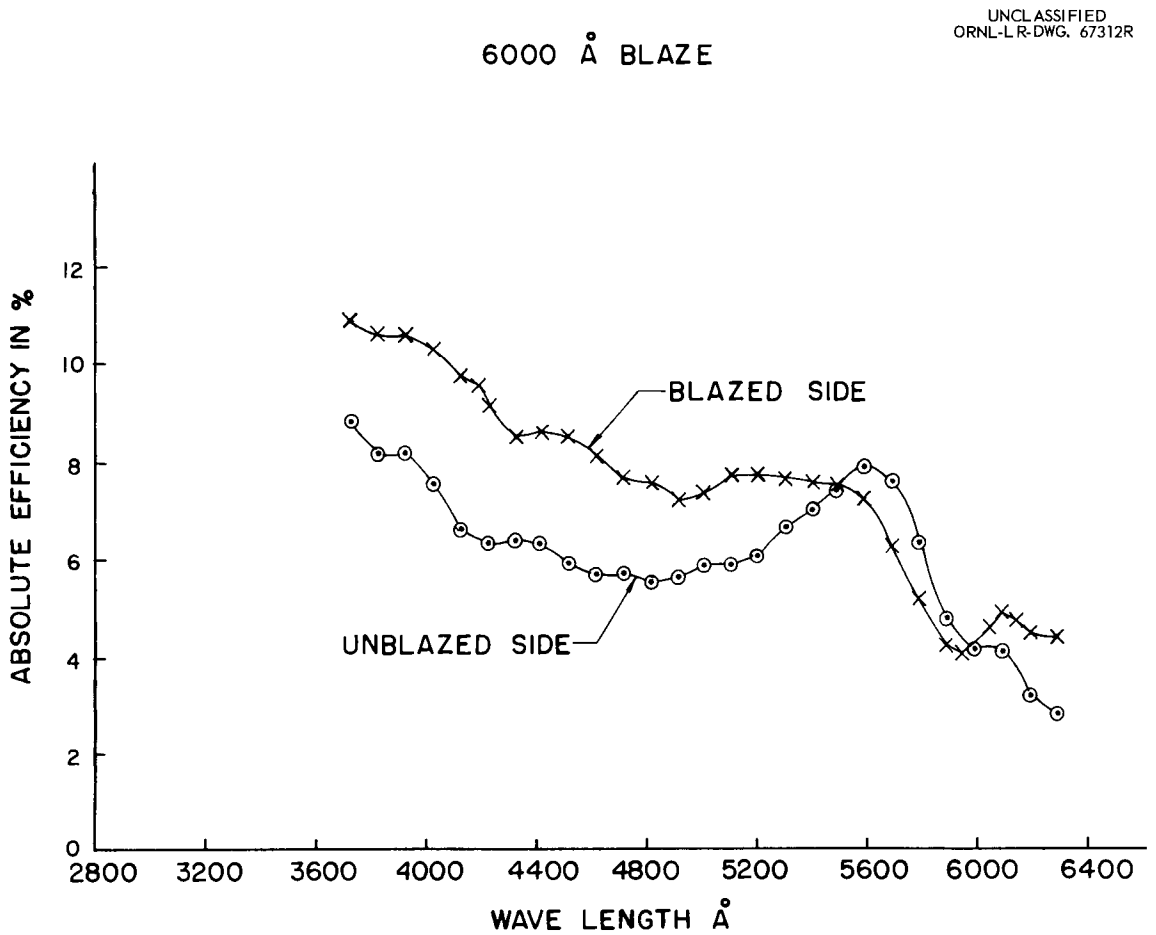


Fig. 9.—Absolute efficiency of 6000-Å blaze grating as a function of wavelength.

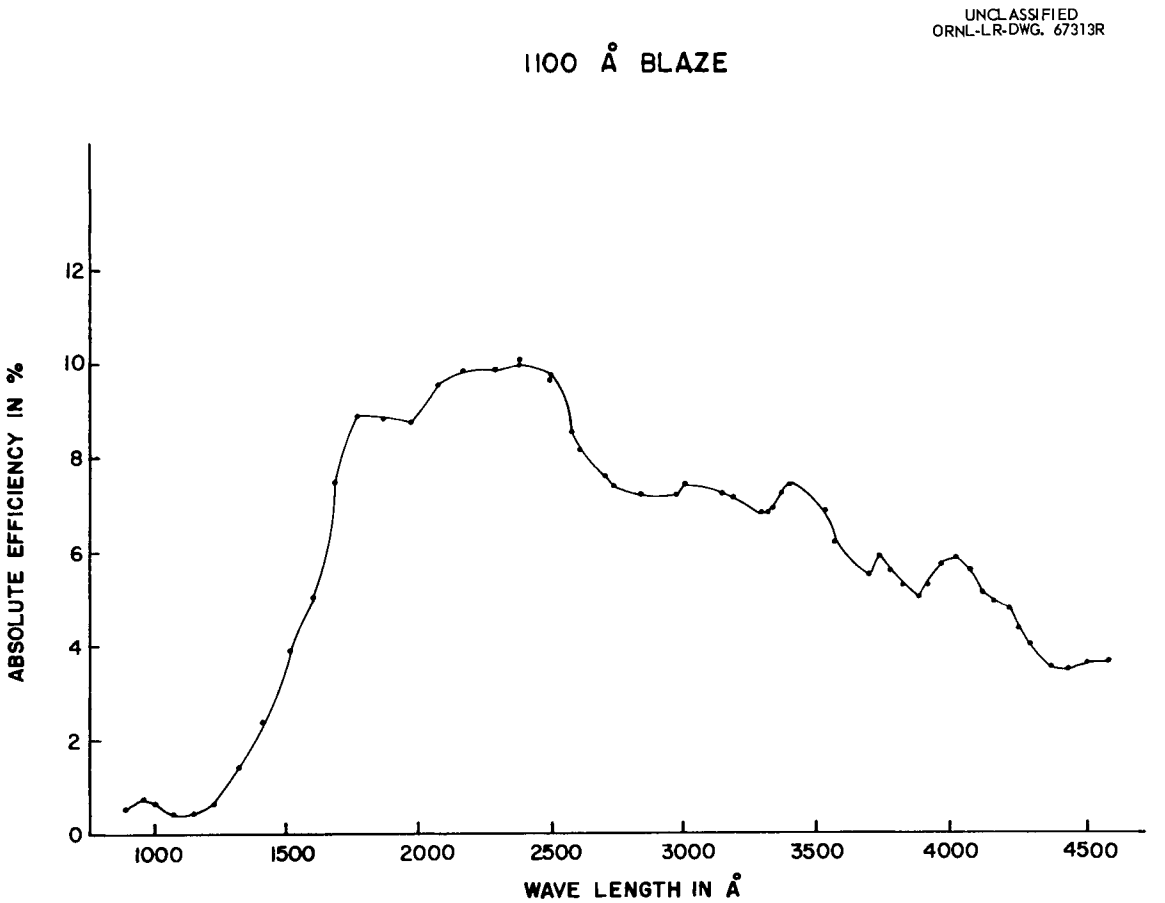


Fig. 10.—Absolute efficiency of 1100-Å blaze grating as a function of wavelength.

# VI. RESULTS

The results obtained for the 340-Å foil are shown in Figures 11 through 14 and for the 530-Å foil in Figures 15 through 19. Each experimental curve is the average of three separate runs. The spectral distribution curves have all been corrected on an absolute intensity scale for the response of the detection system. The theoretical curves, plotted on the same absolute scale, were calculated from Equation (2). The optical constants of Au required in the calculations were taken from the results of R. Philip.[27]

Good agreement is seen between the theoretical predictions and the experimental results in the parallel plane for both foils. The theoretical prediction of a linear dependence of the intensity on electron energy is verified by the study. The plane of polarization and the spectral distribution of the observed emission follows that of transition radiation theory. The absolute yield agrees with theoretical calculations for the higher energies while at lower energies agreement is poorer, with experimental yields higher than theoretical values by a factor of two or three. However, it should be noted that the perpendicular component increases with decreasing beam energy. The bremsstrahlung calculations of Gluckstern, Hull, and Breit predict an increase of this kind with decreasing beam energy, as shown in Figure 20 for a 500-Å foil. The experimental points in the perpendicular plane at the various beam energies are also plotted. The relative

---

[26] Philip, loc. cit.

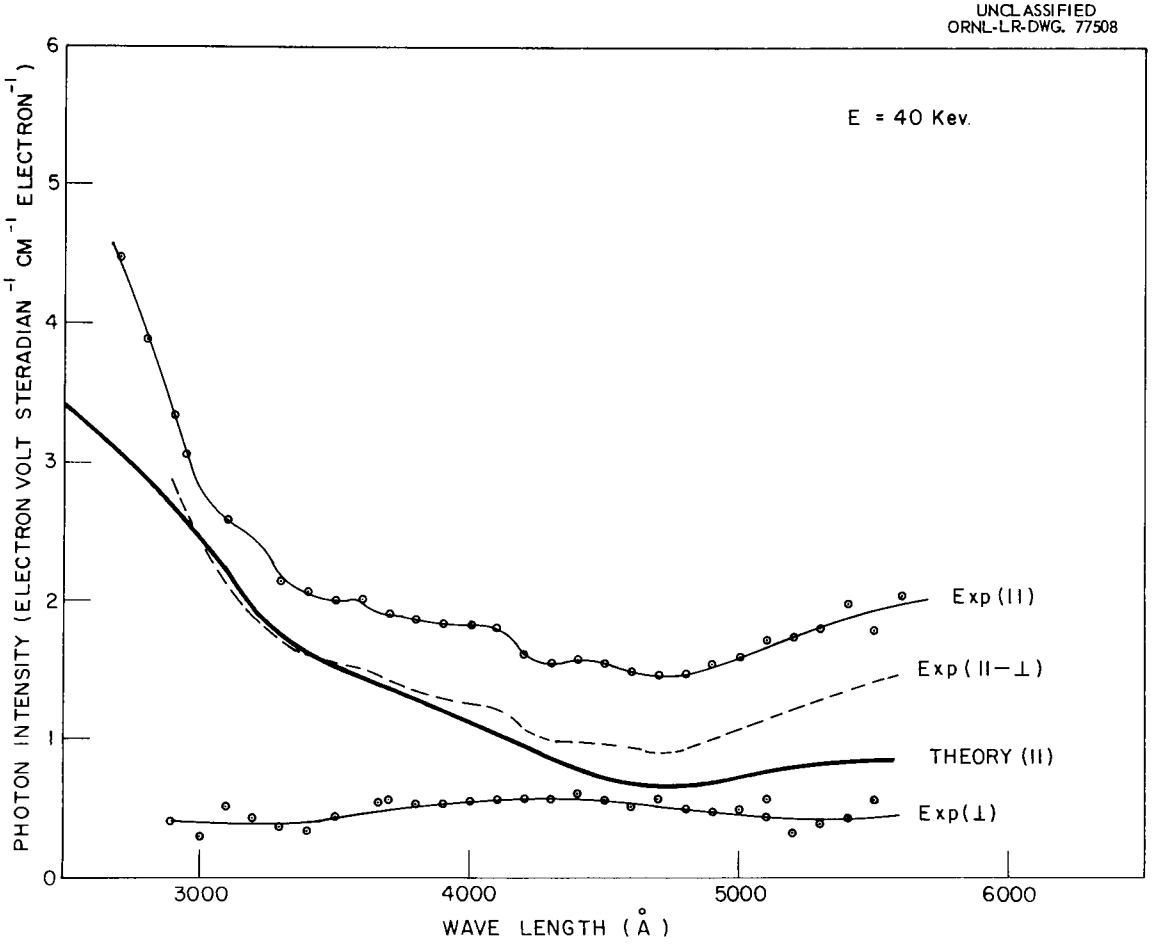


Fig. 11.—Spectral distributions for 340-Å Au foil (E = 40 kev).

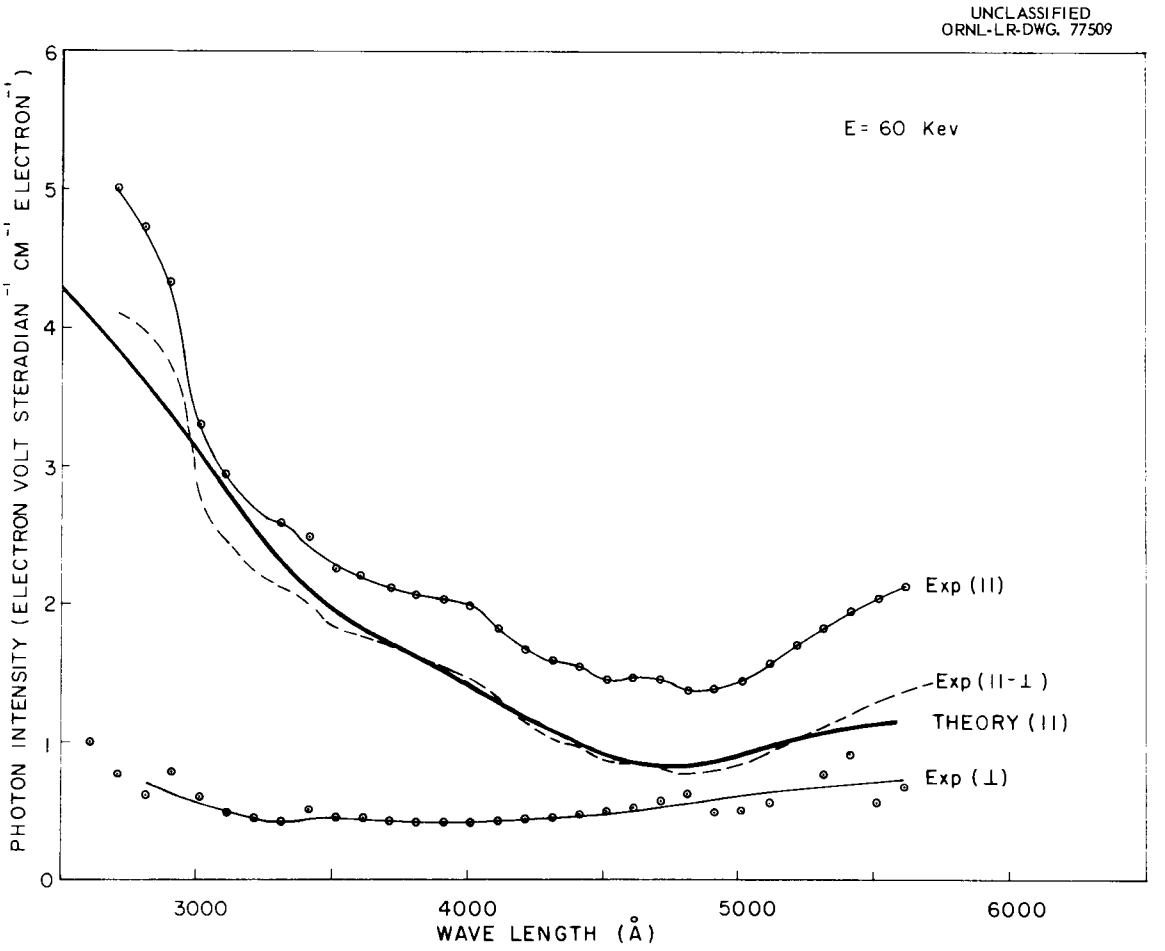


Fig. 12.—Spectral distributions for 340-Å Au foil (E = 60 kev).

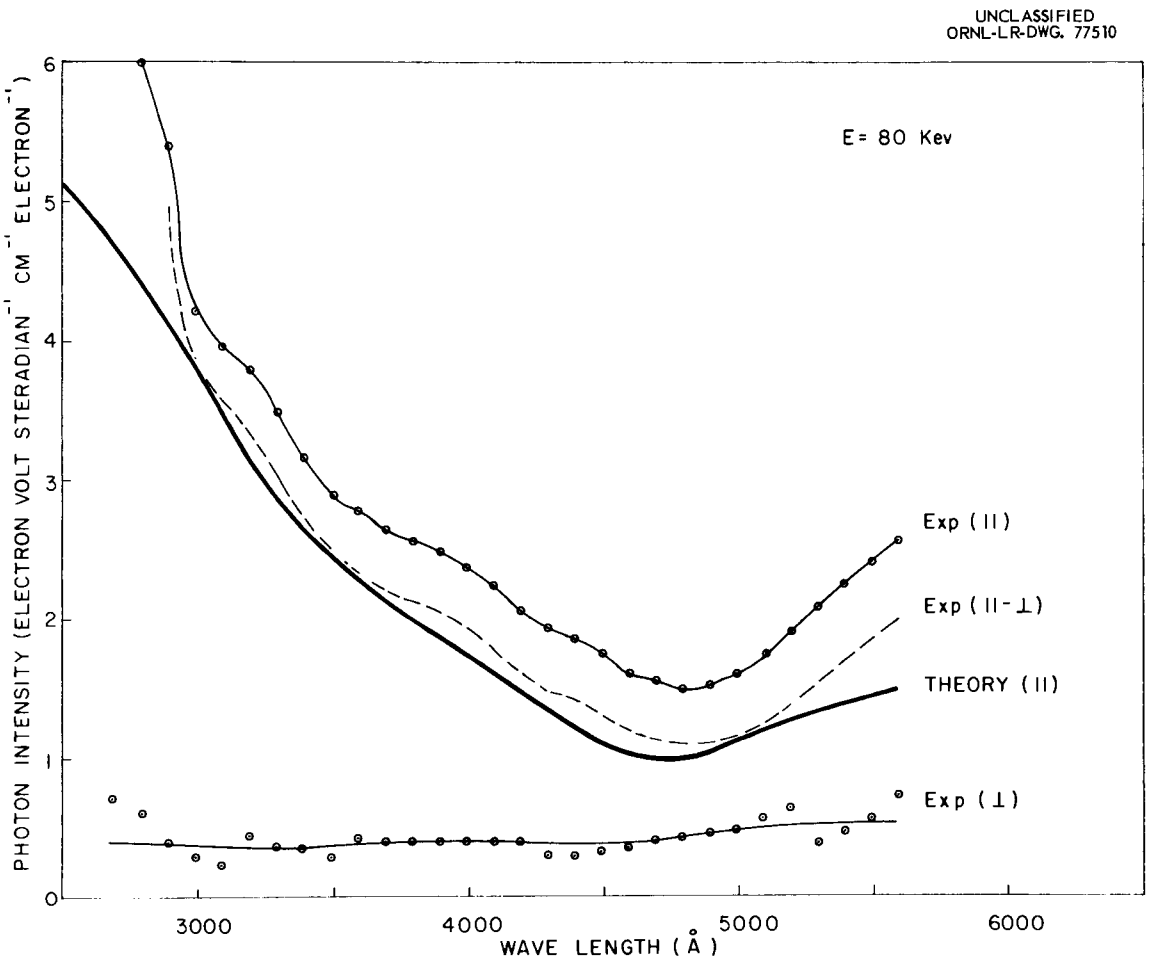


Fig. 13.—Spectral distributions for 340-Å Au foil (E = 80 kev).

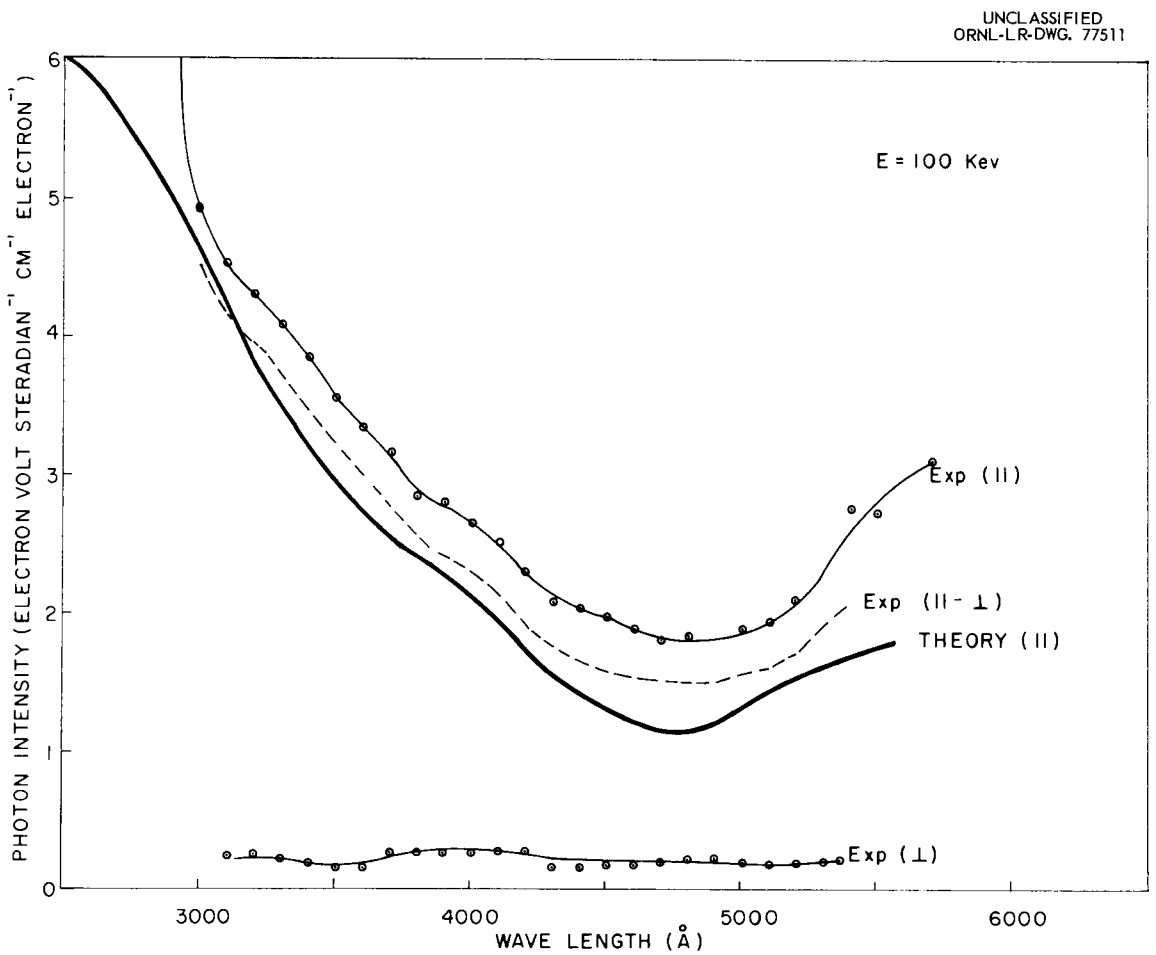


Fig. 14.—Spectral distributions for 340-Å Au foil (E = 100 kev).

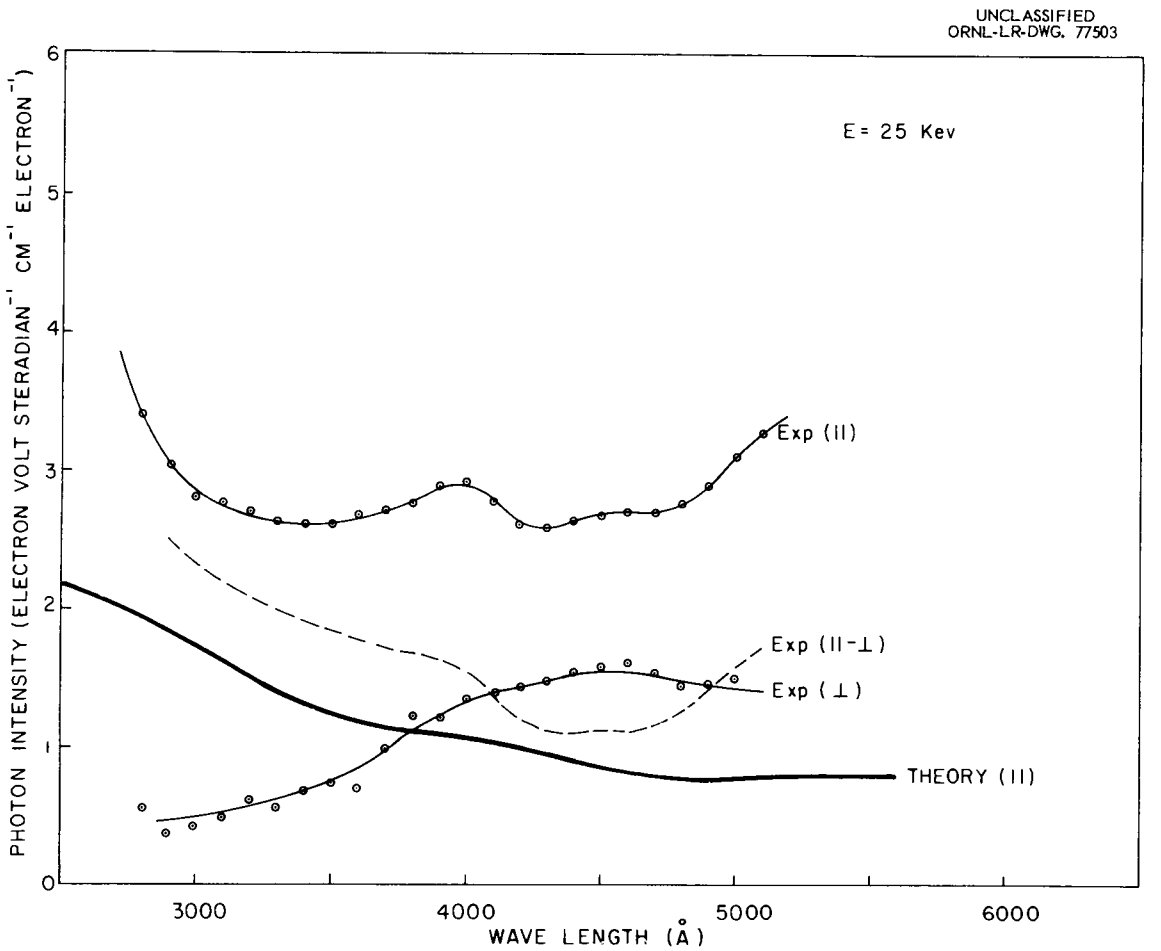


Fig. 15.—Spectral distributions for 530-Å Au foil (E = 25 kev).

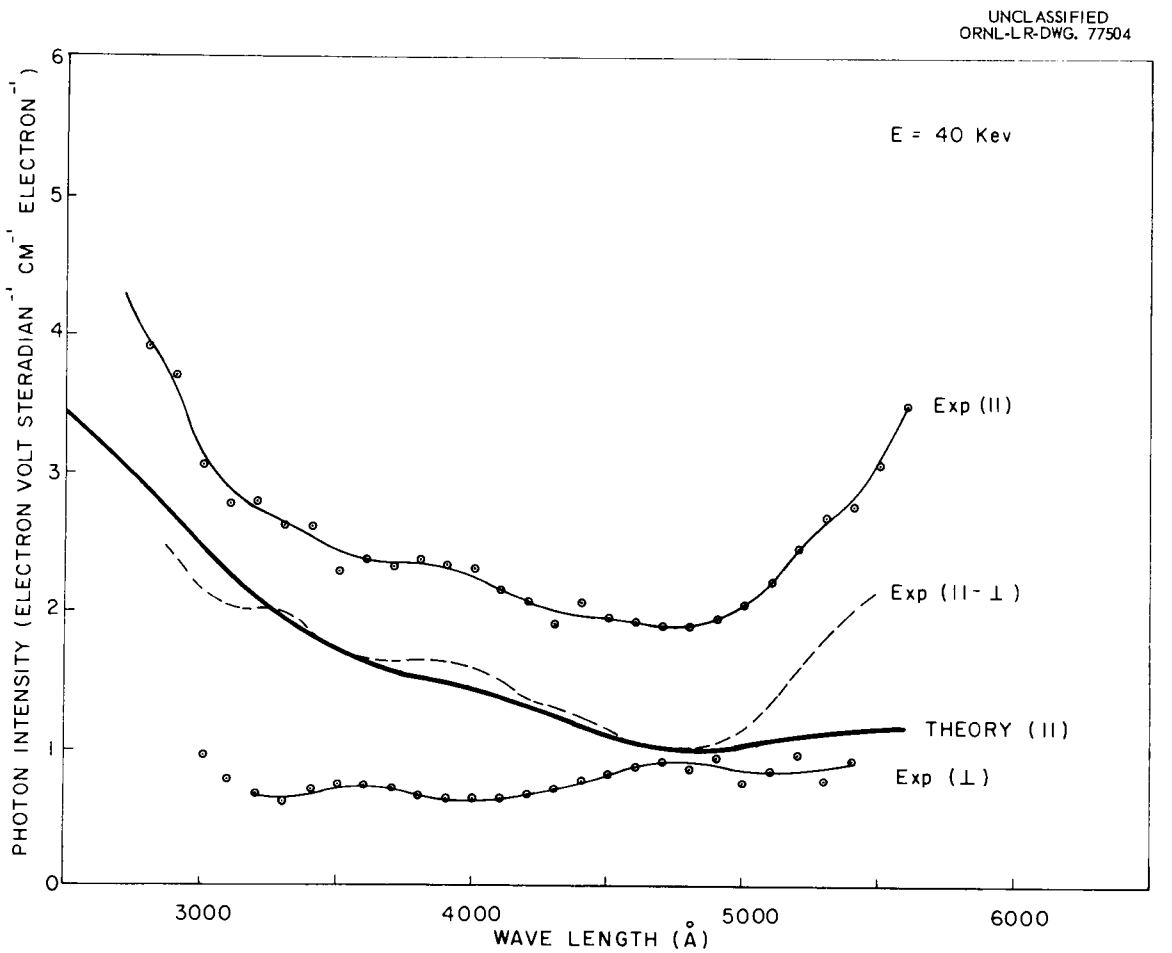


Fig. 16.—Spectral distributions for 530-Å Au foil (E = 40 kev).

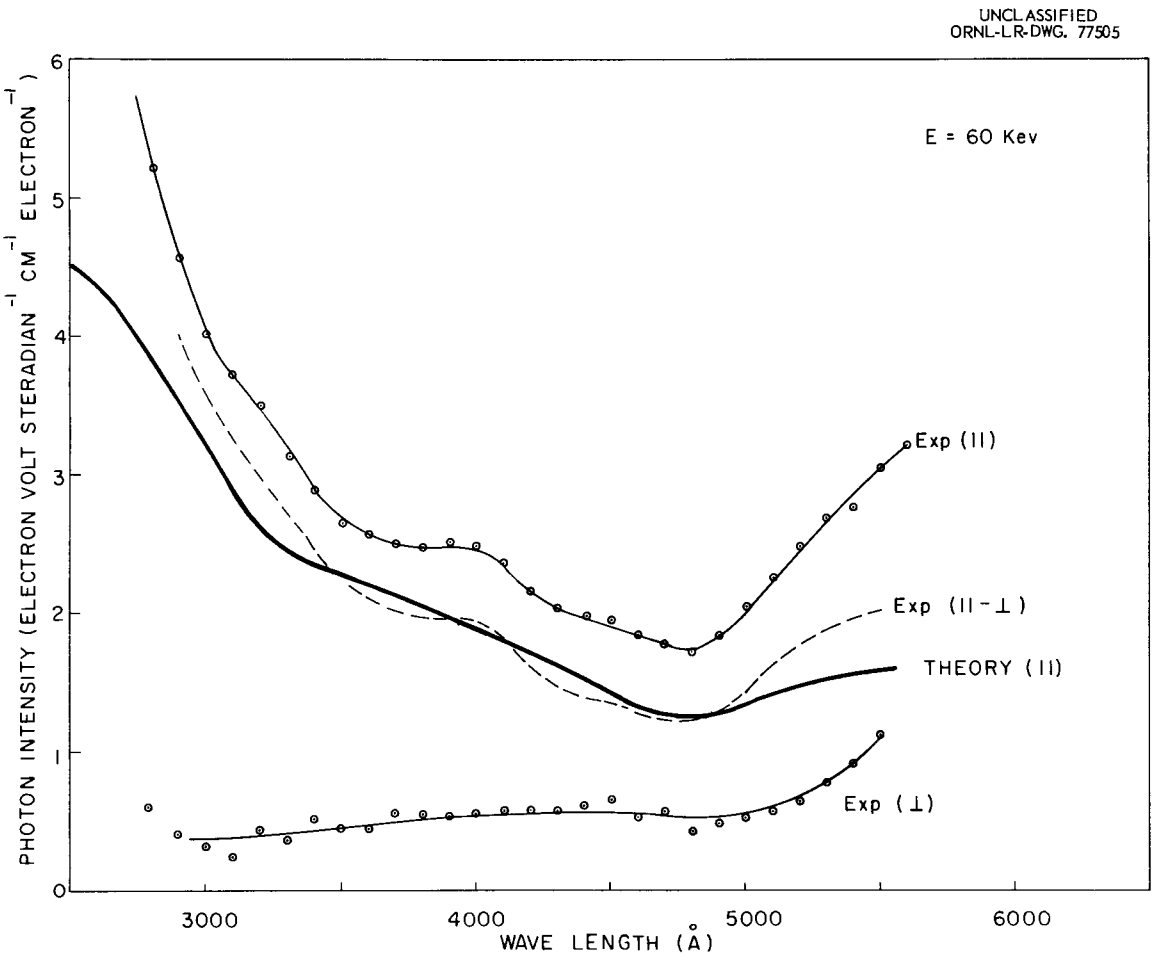


Fig. 17.—Spectral distributions for 530-Å Au foil (E = 60 kev).

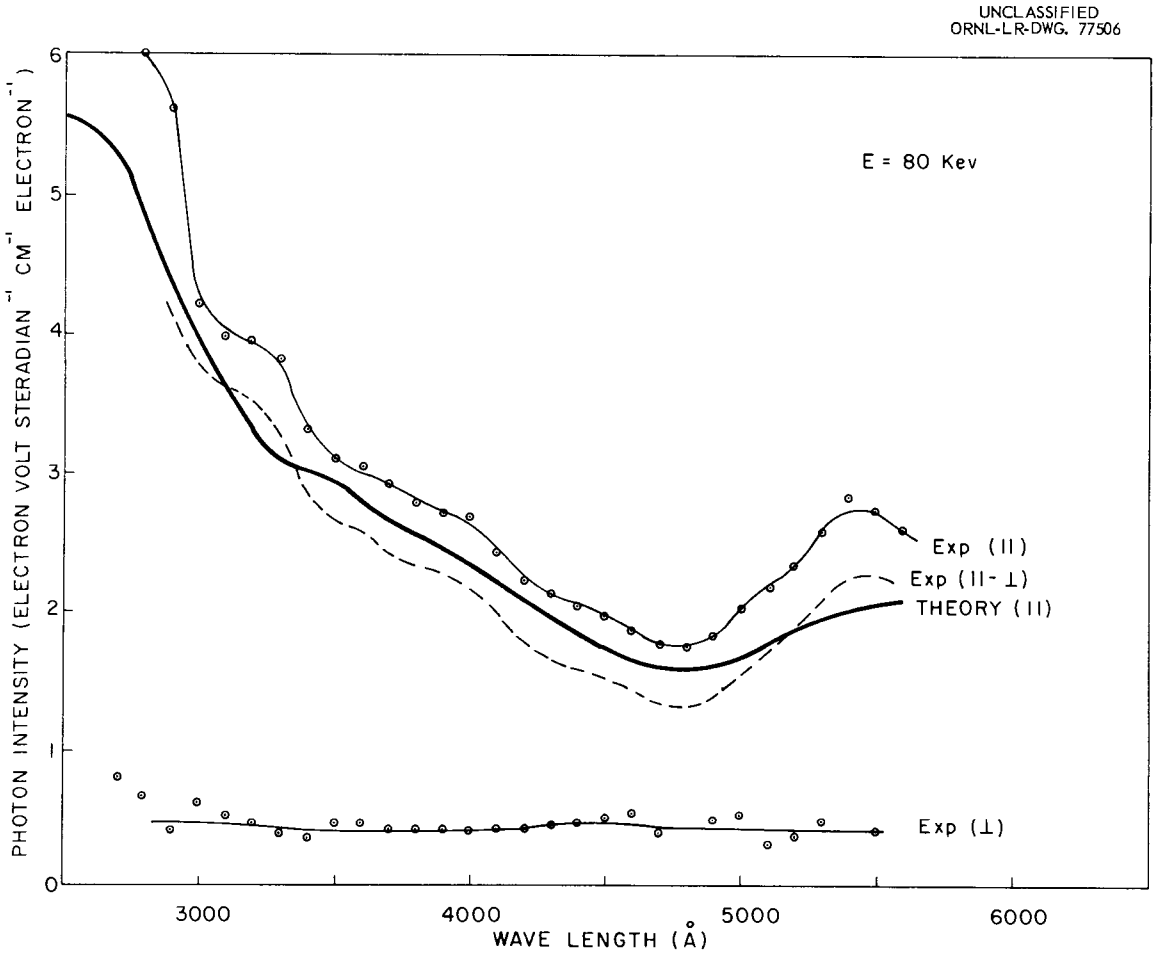


Fig. 18.—Spectral distributions for 530-Å Au foil (E = 80 kev).

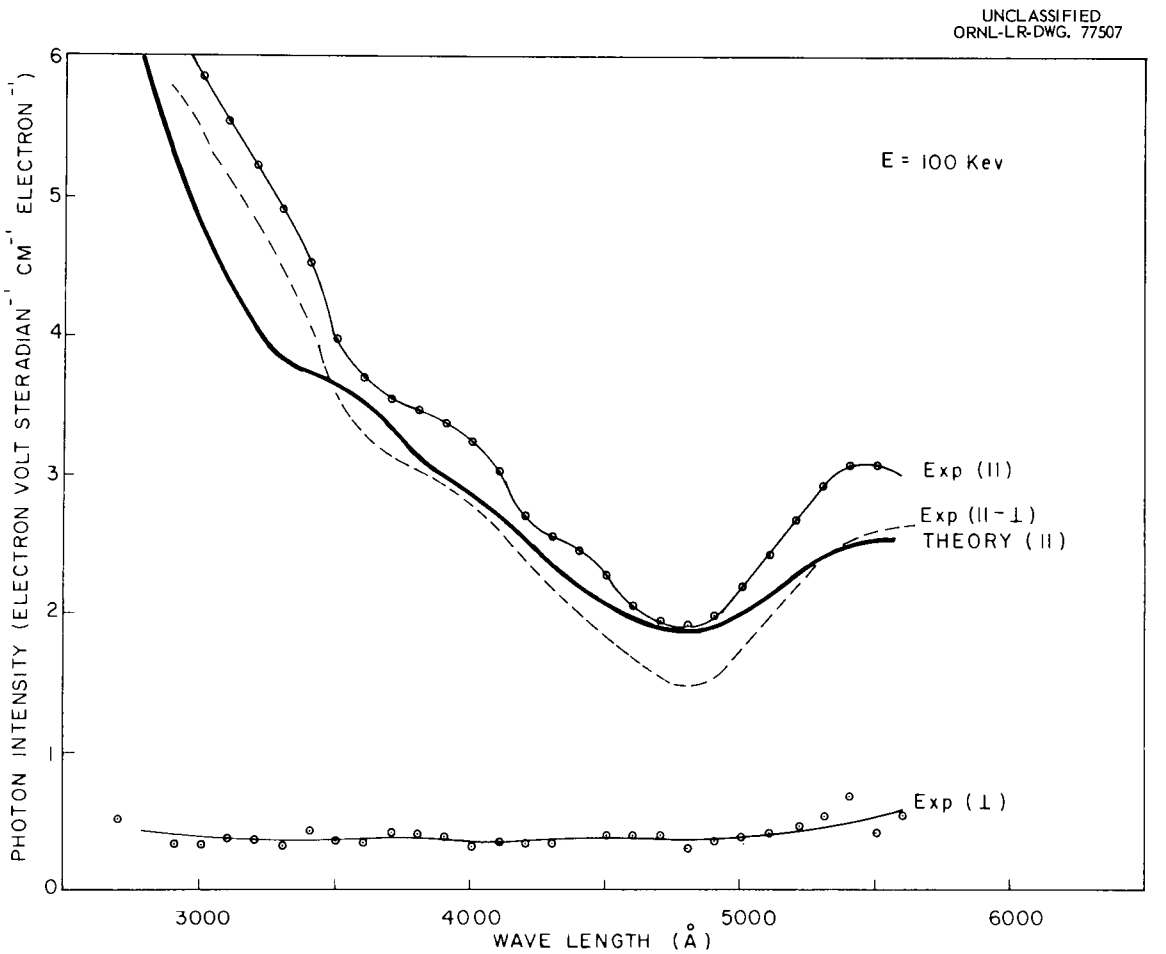


Fig. 19.—Spectral distributions for 530-Å Au foil (E = 100 kev)

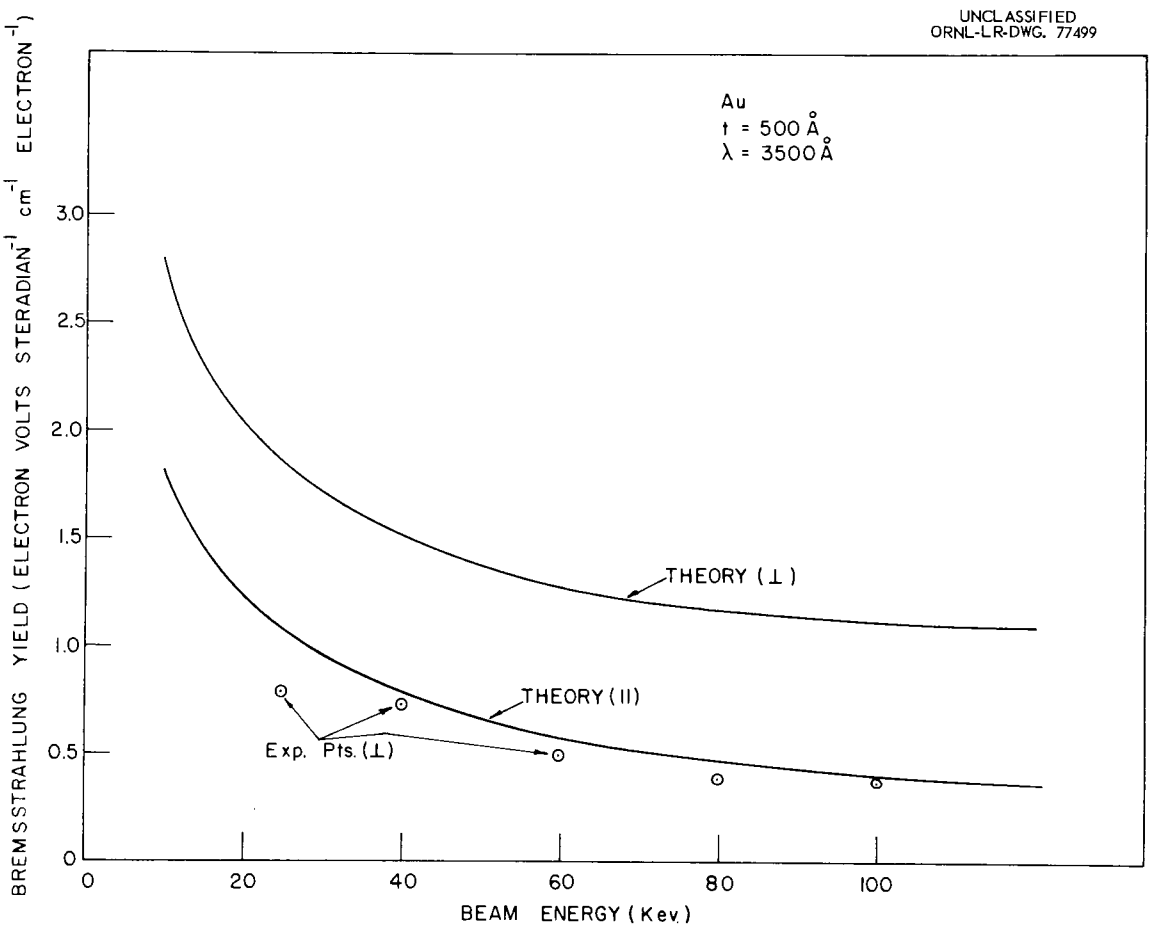


Fig. 20.—Bremsstrahlung yield for gold as a function of beam energy ($t$ = 500 Å, $\lambda$ = 3500 Å)

dependence of the yield on energy agrees well with theory, although the experimental yield is only 40% of the theoretical value. The experimental yield is expected to be lower because the theoretical value is for isolated atoms without regard for the refraction and absorption of the bremsstrahlung photons in the medium. The experimentally observed emission in the parallel plane contains not only transition radiation but also the parallel component of bremsstrahlung. Therefore, the spectral distribution curves were analyzed initially by subtracting from the experimental intensity in the parallel plane $I_{\parallel}$, the quantity $\left[\frac{d\sigma_{\parallel}}{d\sigma_{\perp}}\right] I_{\perp}$ where $d\sigma_{\parallel}$ and $d\sigma_{\perp}$ are given by Equations (3) and (4), and the quantity $I_{\perp}$ is the intensity observed experimentally in the perpendicular plane. An analysis of the spectra in the parallel plane in this fashion showed a little better agreement with transition radiation theory. However, better agreement still was obtained with the quantity $I_{\parallel}-I_{\perp}$ as shown by the dashed curves in Figures 11 through 19. The agreement between transition radiation theory and experiment is now seen to be good for all energies, whereas before this correction, agreement was obtained only for the higher beam energies. The interpretation of the data in this way suggests that the observed bremsstrahlung is unpolarized. The calculations of Gluckstern, Hull, and Breit for isolated atoms show the ratio $\left[\frac{d\sigma_{\parallel}}{d\sigma_{\perp}}\right]$ to be approximately 0.5 for the condition of this experiment. The dielectric response of the medium will increase this ratio because the light transmitted through such a medium is preferentially polarized in the plane of incidence. This effect will raise the intensity in the parallel plane, and thus the

ratio $\left[\frac{d\sigma_{\parallel}}{d\sigma_{\perp}}\right]$ will be greater than 0.5 and may be of the order of unity as implied by the experiments. Calculations of the bremsstrahlung yield which include the effects of refraction and absorption of photons in a dielectric medium are presently being carried out at this Laboratory.

# VII. REVIEW AND CONCLUSIONS

The present investigations of the light emitted by gold foils bombarded by a high energy electron beam substantiate the predictions of transition radiation theory in absolute yield and spectral distribution as a function of electron energy and foil thickness. They also prove the feasibility of an experimental investigation of bremsstrahlung in the optical region where it has not been studied previously.

The experimental results show that gold emits a continuous distribution of photons polarized parallel to the plane of incidence over the spectral region investigated. The spectrum is characterized by a fairly rapid decrease in photon intensity at the shorter wavelengths to a minimum at 4500 Å to 5000 Å followed by a gradual rise to 5500 Å. In general, the measured intensities fall in the range from 1 to 10 eV per incident electron per unit solid angle per centimeter of wavelength. The spectral distribution of photons polarized perpendicular to the plane of incidence was found to be fairly flat with intensities ranging from 10% to 20% of those of the parallel component.

The experimental results were compared with the generalized theory of transition radiation as formulated by Ritchie and Eldridge and with the low energy bremsstrahlung theory of Gluckstern, Hull, and Breit. The agreement between the measured intensities of the parallel polarized components and the calculated intensities of transition radiation was found to be good, especially at the higher energies. The experimentally measured perpendicular components were compared with the calculated perpendicular components of optical bremsstrahlung. Although

the absolute agreement was not as good in the case of transition radiation, the inverse energy dependence predicted by the Gluckstern-Hull-Breit theory was observed. Reasons for the observed discrepancies are presented.

The results obtained with the grating calibrator show that misleading conclusions may be reached in the interpretation of continuous emission spectra (i.e., small spectral "humps" may be interpreted as emission peaks, whereas they are actually due to anomalous grating efficiency maxima) unless a careful analysis of the complete detection system is made. The calibration has proven valuable in these low intensity experiments by showing that an increase in intensity by a factor of ten could be obtained at the detector by a simple change of grating in the spectrometer from JA6000 to BL-3500. Using the techniques described, it appears feasible to study the emission of light from electron-bombarded foils in the spectral region from 500 Å to 2500 Å on an absolute basis.

# BIBLIOGRAPHY


Arakawa, E. T., Frank, A. L., Birkhoff, R. D., and Ritchie, R. H., "Optical Emission of Irradiated Ag and Al Foils," Bull. Am. Phys. Soc. 6, 266 (1961).

Ferrell, R. A., "Predicted Radiation of Plasma Oscillations in Metal Films," Phys. Rev. 111, 1214-1222 (1958).

Frank, A. L., Birkhoff, R. D., Arakawa, E. T., Ritchie, R. H., and Eldridge, H. B., "Optical Emission from Irradiated Thin Metallic Foils," Oak Ridge National Laboratory Report ORNL-3114, 1962.

Frank, I. M., "Transition Radiation and the Cherenkov Effect," Uspekhi Fiz. Nauk. 75, 231-240 (1961).

Frank, I. M., and Ginzburg, V., "Radiation of a Uniformly Moving Electron Due to its Transition from One Medium into Another," J. Phys. (U.S.S.R.) 9, 353-362 (1945).

Gluckstern, R. L., Hull, M. H., Jr., and Breit, G., "Polarization of Bremsstrahlung Radiation," Phys. Rev. 90, 1026-1029 (1953).

Hammer, D. C., Arakawa, E. T., and Birkhoff, R. D., "A Simple Grating Calibrator for the Visible and Vacuum Ultraviolet," to be published in Applied Optics.

Holland, L., Vacuum Deposition of Thin Films (John Wiley and Sons, Inc., New York, 1960).

Kalil, F., Stone, W. G., Hubbell, H. H., and Birkhoff, R. D., "Stopping Power of Thin Aluminum Foils for 12 to 127 kev Electrons," Oak Ridge National Laboratory Report ORNL-2731, 1959.

Namioka, T., "Theory of the Ellipsoidal Concave Grating. II. Application of the Theory to Specific Grating Mountings," J. Opt. Soc. Am. 51, 13-16 (1961).

Neugebauer, C. A., Newkirk, J. B., and Vermilyea, D. A. (Eds.), Structure and Properties of Thin Films (John Wiley and Sons, Inc., New York, 1959).

Philip, R., "Constantes Optiques et Variations de Phase de L'or en Couches Minces," Opt. Acta 7, 47-52 (1960).

Ritchie, R. H., and Eldridge, H. B., "Optical Emission from Irradiated Foils. I," Phys. Rev. 126, 1935-1947 (1962).

Stair, R., Johnston, R. G., and Halbach, E. W., "Standard of Spectral Radiance for the Region of 0.25 to 2.6 Microns," J. Research Natl. Bur. Standards 64A, 291-296 (1960).

Tolansky, S., An Introduction to Interferometry (Longmans, Green and Co., London, 1955).

Tolansky, S., Surface Microtopography (Interscience Publishers, Inc., New York, 1960).

Watanabe, K., and Inn, Edward C. Y., "Intensity Measurements in the Vacuum Ultraviolet," J. Opt. Soc. Am. 43, 32-35 (1953).

Ziemer, P. L., Johnson, R. M., and Birkhoff, R. D., "Measurement of Stopping Power of Copper by Calorimetric Methods," Oak Ridge National Laboratory Report ORNL-2775, 1959.

ORNL-3468
UC-34 -- Physics
TID-4500 (21st ed.)

## INTERNAL DISTRIBUTION

1. Biology Library
2-4. Central Research Library
5. Reactor Division Library
6-7. ORNL -- Y-12 Technical Library
8-57. Laboratory Records Department
58. Laboratory Records, ORNL R. C.
59-83. E. T. Arakawa
84. J. A. Auxier
85. P. S. Baker
86-110. R. D. Birkhoff
111-135. L. C. Emerson
136. H. H. Hubbell
137-146. G. S. Hurst
147. W. H. Jordan
148. B. H. Ketelle
149. C. E. Larson
150. K. Z. Morgan
151. W. F. Mruk
152. D. R. Nelson
153. R. H. Ritchie
154. R. L. Shipp
155. M. J. Skinner
156. J. A. Swartout
157. A. M. Weinberg
158. G. M. Fair (Consultant)
159. J. C. Frye (Consultant)
160. W. H. Langham (Consultant)
161. E. P. Odum (Consultant)
162. R. L. Platzman (Consultant)
163. L. S. Taylor (Consultant)

## EXTERNAL DISTRIBUTION

164-168. D. C. Hammer, NASA Lewis Research Center, Cleveland 35, Ohio
169. N. F. Barr, Division of Biology and Medicine, U. S. Atomic Energy Commission, Washington
170. S. A. Lough, Division of Biology and Medicine, U. S. Atomic Energy Commission, Washington
171. W. Steinman, II. Physikalisches Institut der Universitat, Munchen, Muchen 13, Germany
172. Ye-Yung Teng, Department of Physics and Astronomy, University of Maryland, College Park, Maryland
173. G. L. Weissler, University of Southern California, Department of Physics, Los Angeles 7, California
174. P. R. Wessel, U. S. Naval Ordnance Laboratory, Silverspring, Maryland
175. R. W. Wood, Division of Biology and Medicine, U. S. Atomic Energy Commission, Washington
176. Professor V. B. Bhanot, Physics Department, Panjab University, Chandigarh-3, India
177. Research and Development Division, AEC, ORO
178-740. Given distribution as shown in TID-4500 (21st ed.) under Physics category